Article

Cancer Cell

γ-Catenin-Dependent Signals Maintain BCR-ABL1+ B Cell Acute Lymphoblastic Leukemia

Graphical Abstract

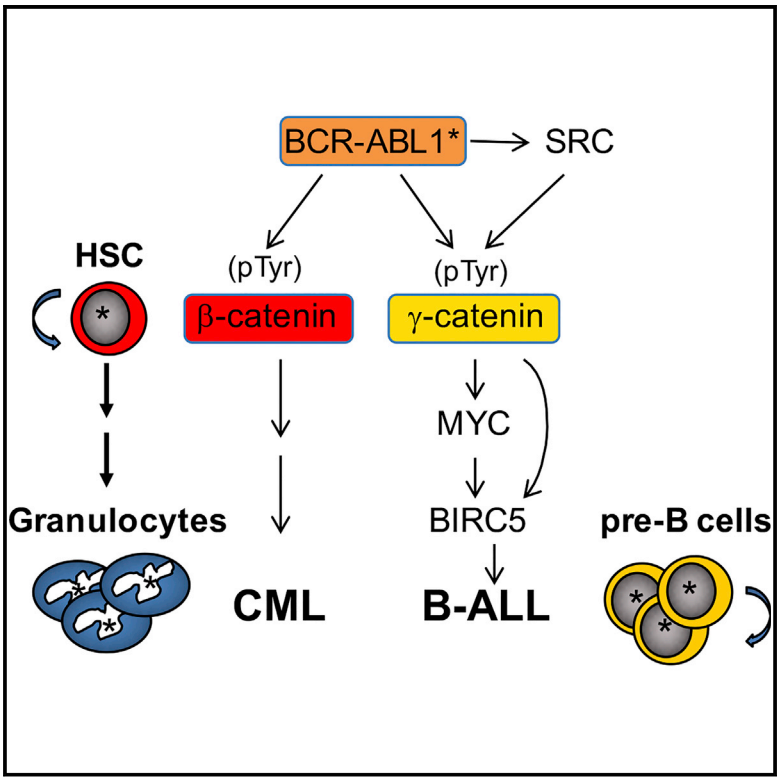

Authors

Noemie Luong-Gardiol, Imran Siddiqui, Irene Pizzitola, ..., Jean-Pierre Bourquin, Joerg Huelsken, Werner Held

Correspondence

werner.held@unil.ch

In Brief

Luong-Gardiol et al. show that Wnt pathway activity mediated by γ-catenin is critical for BCR-ABL1+ B-ALL, in contrast to β-catenin being important in CML. B-ALL is more sensitive to partial reduction of MYC expression level than CML, and γ-catenin regulates the expression of MYC and Survivin in B-ALL.

Highlights

- Maintenance of BCR-ABL1+ B-ALL depends on γ-catenin (Junction plakoglobin)
- γ-Catenin and β-catenin play selective roles in BCR-ABL1+ B-ALL and CML, respectively
- MYC and BIRC5 (Survivin) are essential targets of γ-catenin in BCR-ABL1+ B-ALL
- ABL kinase inhibitor-resistant B-ALL cells are susceptible to γ-catenin suppression

Luong-Gardiol et al., 2019, Cancer Cell *35*, 649–663
April 15, 2019
https://doi.org/10.1016/j.ccell.2019.03.005

CellPress

Cancer Cell
Article

γ-Catenin-Dependent Signals Maintain BCR-ABL1$^+$ B Cell Acute Lymphoblastic Leukemia

Noemie Luong-Gardiol,[1,7,10] Imran Siddiqui,[1,10] Irene Pizzitola,[1,10] Beena Jeevan-Raj,[1,10] Mélanie Charmoy,[1,10] Yun Huang,[2] Anja Irmisch,[3,8] Sara Curtet,[1] Georgi S. Angelov,[1] Maxime Danilo,[1,9] Mélanie Juilland,[4] Beat Bornhauser,[2] Margot Thome,[4] Oliver Hantschel,[3] Yves Chalandon,[5] Gianni Cazzaniga,[6] Jean-Pierre Bourquin,[2] Joerg Huelsken,[3] and Werner Held[1,11,*]

[1]Department of Oncology UNIL CHUV, University of Lausanne, Epalinges, Switzerland
[2]Department of Pediatric Oncology and Children's Research Centre, University Children's Hospital Zürich, Zürich, Switzerland
[3]Swiss Institute for Experimental Cancer Research (ISREC), Federal University of Technology Lausanne (EPFL), Lausanne, Switzerland
[4]Department of Biochemistry, University of Lausanne, Epalinges, Switzerland
[5]Service d'Hématologie, Hôpitaux Universitaire de Genève, Geneva, Switzerland
[6]Centro Ricerca Tettamanti, Pediatric Clinic University of Milano-Bicocca, Monza, Italy
[7]Present address: Debiopharm International SA, Ch. Messidor 5–7, 1002 Lausanne, Switzerland
[8]Present address: University Hospital Zürich, Clinic of Dermatology, Wagistrasse 14, 8952 Schlieren, Switzerland
[9]Present address: Phi Pharma SA, Place du Midi 36, 1950 Sion, Switzerland
[10]These authors contributed equally
[11]Lead Contact
*Correspondence: werner.held@unil.ch
https://doi.org/10.1016/j.ccell.2019.03.005

SUMMARY

The BCR-ABL1 fusion protein is the cause of chronic myeloid leukemia (CML) and of a significant fraction of adult-onset B cell acute lymphoblastic leukemia (B-ALL) cases. Using mouse models and patient-derived samples, we identified an essential role for γ-catenin in the initiation and maintenance of BCR-ABL1$^+$ B-ALL but not CML. The selectivity was explained by a partial γ-catenin dependence of MYC expression together with the susceptibility of B-ALL, but not CML, to reduced MYC levels. MYC and γ-catenin enabled B-ALL maintenance by augmenting BIRC5 and enforced BIRC5 expression overcame γ-catenin loss. Since γ-catenin was dispensable for normal hematopoiesis, these lineage- and disease-specific features of canonical Wnt signaling identified a potential therapeutic target for the treatment of BCR-ABL1$^+$ B-ALL.

INTRODUCTION

The Philadelphia chromosome (Ph), which encodes the BCR-ABL1 fusion protein, is the cause of chronic myeloid leukemia (CML) and of 30% of adult-onset B cell acute lymphoblastic leukemia (B-ALL) cases. Small-molecule tyrosine kinase inhibitors of the constitutively active BCR-ABL1 can effectively control chronic phase CML, but are not curative. Moreover, a significant fraction of CML patients responds poorly to tyrosine kinase inhibitor treatment due to mutations in BCR-ABL1. Even worse, Ph$^+$ B-ALL patients only transiently respond to inhibitor treatment and have a poor prognosis (Hunger, 2011; O'Hare et al., 2012). Thus additional therapeutic targets are needed to control and eventually cure Ph$^+$ leukemia.

Mouse models revealed that CML originates from long-term hematopoietic stem cells (LT-HSC) and is propagated by LT-HSC-like leukemia-initiating cells (LIC) (Huntly et al., 2004), which are resistant to inhibitor treatment (Hu et al., 2006). Thus BCR-ABL1 exploits the self-renewal capacity of LT-HSC for the sustained overproduction of mature myeloid cells. In contrast, the cancer-propagating cell for B-ALL resembles pro-B cells (Signer et al., 2010), and multiple developmental stages

Significance

Philadelphia chromosome-positive (Ph$^+$) (BCR-ABL1$^+$) B cell acute lymphoblastic leukemia (B-ALL) has a high relapse rate after combined treatment with tyrosine kinase inhibitors and chemotherapy, highlighting a need for the identification of additional therapeutic targets. We have identified γ-catenin as a key component of a signaling cascade downstream of BCR-ABL1, which maintained Ph$^+$ B-ALL by sustaining the expression of the critical downstream targets MYC and BIRC5 (Survivin). Since targeting γ-catenin overcame the resistance of Ph$^+$ B-ALL cells to ABL kinase inhibitors and γ-catenin expression was not essential for steady-state hematopoiesis, our findings identified a potential therapeutic target, which may circumvent the likely side effects of a global inhibition of the canonical Wnt pathway.

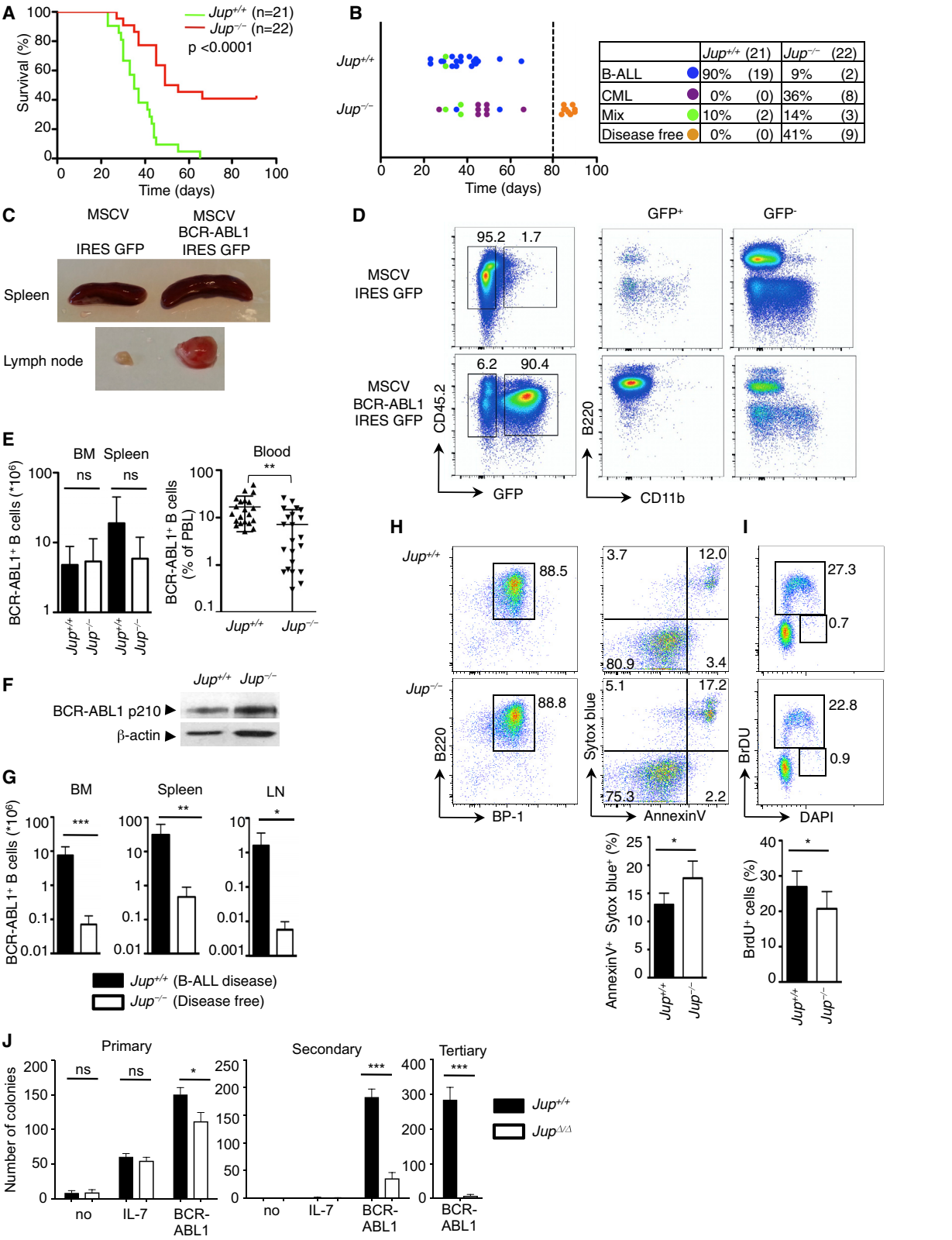

(legend on next page)

can serve as a cell of origin for B-ALL, including LT-HSC, common lymphoid progenitors, and lineage-restricted pro-B cells (Kovacic et al., 2012; Signer et al., 2010). The BCR-ABL1 mediated self-renewal of lineage-committed B cells is poorly understood.

Self-renewal and differentiation of hematopoietic stem and progenitor cells is associated with canonical Wnt signals. Aberrantly increased expression of Wnt pathway components is observed in various types of leukemia (Jamieson et al., 2004; Lu et al., 2004) and abnormal Wnt/β-catenin signaling has a critical role in multiple myeloma (Yeung et al., 2010), acute myeloid leukemia (AML) (Wang et al., 2010), and CML (Hu et al., 2009; Schurch et al., 2012; Zhao et al., 2007). Indeed, β-catenin (encoded by *Ctnnb1*) plays an essential role for the generation (Zhao et al., 2007) and the maintenance of CML LIC (Heidel et al., 2012) and their resistance to tyrosine kinase inhibitors (Hu et al., 2009). While β-catenin-deficiency largely prevented the induction of CML by BCR-ABL1, recipient mice instead succumbed to B-ALL (Zhao et al., 2007). BCR-ABL1$^+$ lymphocytic leukemia may thus not depend on the Wnt pathway or depend on the alternative Wnt signal transducer γ-catenin (Junction plakoglobin, encoded by *JUP*). Consistent with a possible role in leukemia, γ-catenin expression is frequently upregulated in AML (Morgan et al., 2012; Muller-Tidow et al., 2004; Zheng et al., 2004), and enforced expression of γ-catenin in hematopoietic progenitors induced a myeloproliferative syndrome (Zheng et al., 2004). However, it has not been known whether γ-catenin is essential for leukemia initiation or maintenance and, if so, whether there exist lineage-specific roles for γ-catenin and/or β-catenin.

RESULTS

γ-Catenin Is Essential for Initiating Ph$^+$ B-ALL

To investigate whether γ-catenin played a role for B-ALL development, we used bone marrow (BM) from γ-catenin-deficient (*Jup*$^{-/-}$) and wild-type (WT, *Jup*$^{+/+}$) fetal liver chimeras (CD45.2) (Figure S1A). Infection of total BM cells with a retrovirus encoding BCR-ABL1 (p210) and GFP lead to the preferential transduction of B220$^+$ cells (Figure S1B). Following transplantation into irradiated C57BL/6 (B6) mice (CD45.1), most recipients receiving *Jup*$^{+/+}$ BM (90%) developed B-ALL (Figures 1A and 1B), which was characterized by frequent hind leg paralysis, moderate splenomegaly, pleural effusion, enlarged lymph nodes (Figure 1C), and expansions of cells with a pre-B cell phenotype (B220$^+$CD43^{dim}CD19$^+$BP-1$^+$IgM$^-$) in the BM, secondary lymphoid organs, and blood of recipients (Figure 1D and data not shown) (Roumiantsev et al., 2001). The remaining recipients (10%) showed mixed B-ALL/myeloid expansions, with symptoms characteristic of B-ALL rather than CML-like disease (see later). In contrast, a significant fraction (41%) of recipients of BCR-ABL1 transduced *Jup*$^{-/-}$ BM did not develop disease for >80 days (Figures 1A and 1B). While a few of the remaining recipients developed B-ALL (9%), some showed a mixed B-ALL/myeloid phenotype (14%) and a larger fraction succumbed to CML-like disease (36%) (Figure 1B). Thus, B-ALL initiation by BCR-ABL1 depended on γ-catenin.

Impaired initiation of Ph$^+$ B-ALL was not related to evident perturbations of normal hematopoiesis (Figure S1C) or B cell development in *Jup*$^{-/-}$ chimeras (Figure S1D). Furthermore, *Jup*$^{+/+}$ and *Jup*$^{-/-}$ BM cells were transduced with comparable efficiency (Figure S1E). Between 2 and 3 weeks after transplantation of transduced BM, but prior to the development of overt signs of leukemia (referred to as pre-leukemic stage), we noted comparable populations of BCR-ABL1$^+$ B cells in the BM and spleen of recipient mice although *Jup*$^{-/-}$ B cells were reduced in the blood (Figure 1E). BCR-ABL1$^+$ cells had an identical phenotype (B220$^+$CD43^{dim}BP-1$^+$IgM$^-$) and expressed comparable amounts of BCR-ABL1 protein (Figure 1F). Despite the efficient initial engraftment and expansion, disease-free recipients of *Jup*$^{-/-}$ BM (41%) contained few BCR-ABL1$^+$ pre-B cells 8 weeks after transplantation (Figure 1G), indicating that γ-catenin sustained the expansion of BCR-ABL1$^+$ B cells. Consistent with this observation, BCR-ABL1$^+$ *Jup*$^{-/-}$ pre-B cells were more susceptible to undergo apoptosis and proliferation was modestly reduced compared with WT (Figures 1H and 1I). We further estimated cancer cell self-renewal *in vitro* using serial replating assays. Following primary plating, both WT and *Jup*$^{Lox/Lox}$ *Vav-Cre* (*Jup*$^{Δ/Δ}$) BCR-ABL1$^+$ BM cells readily formed B cell colonies. While WT B cells efficiently formed colonies in subsequent platings, that of *Jup*$^{Δ/Δ}$ cells was progressively reduced (Figure 1J). In all cases colonies were composed of B-lineage cells (data not shown). Thus the transient expansion and impaired progression to B cell leukemia could be accounted for by an impaired proliferative renewal in the absence of γ-catenin.

Transformation of B-Lineage-Committed Progenitors Depends on γ-Catenin Expression

CML arises from HSC expressing BCR-ABL1, but not from more differentiated myeloid progenitors (Huntly et al., 2004). In contrast, B-ALL can arise from B cell lineage-committed progenitors (Kovacic et al., 2012; Signer et al., 2010). In agreement with these findings, BCR-ABL1 transduced purified WT

Figure 1. Impaired B-ALL Initiation in the Absence of γ-Catenin

(A–D) Wild-type (WT) recipients (CD45.1) were transplanted with BCR-ABL1 (p210) (GFP) transduced BM cells from *Jup*$^{+/+}$ or *Jup*$^{-/-}$ chimeras (CD45.2) and recipient mice were analyzed for survival (compiled from four independent experiments) (A), leukemia type (B), appearance of spleen and lymph nodes (C), and presence of donor-derived (CD45.2$^+$) GFP$^+$ (BCR-ABL1$^+$) B220$^+$ CD11b$^-$ B cells in the recipient BM (D).

(E and F) GFP$^+$ (BCR-ABL1$^+$) cells were analyzed 2–3 weeks post transplantation for their abundance (E) and the expression of BCR-ABL1 (F).

(G) Disease-free recipients of *Jup*$^{-/-}$ BM were analyzed >8 weeks after transplantation for the presence of residual GFP$^+$ (BCR-ABL1$^+$) B220$^+$ B cells as compared with recipients of *Jup*$^{+/+}$ BM with B-ALL disease.

(H and I) BCR-ABL1$^+$ (mCherry$^+$) B220$^+$ BP-1$^+$ cells were analyzed 2–3 weeks post transplantation for markers of cell death (H) and cell-cycle progression (I).

(J) BM cells from *Jup*$^{lox/lox}$ *Vav-Cre* (*Jup*$^{Δ/Δ}$) and *Jup*$^{lox/lox}$ (*Jup*$^{+/+}$) mice were cultured in IL-7 or transduced with BCR-ABL1 (p185) and plated in methylcellulose. Primary colonies, all consisting only of B-lineage cells, were harvested and replated. Data are mean number of colonies derived from 10^4 B-ALL cells (secondary and tertiary plating) and are representative of two independent experiments.

Error bars in (E) and (G) to (J) represent SD. *p < 0.05, **p<0.01, ***p < 0.001. ns, not significant (p > 0.05). See also Figure S1.

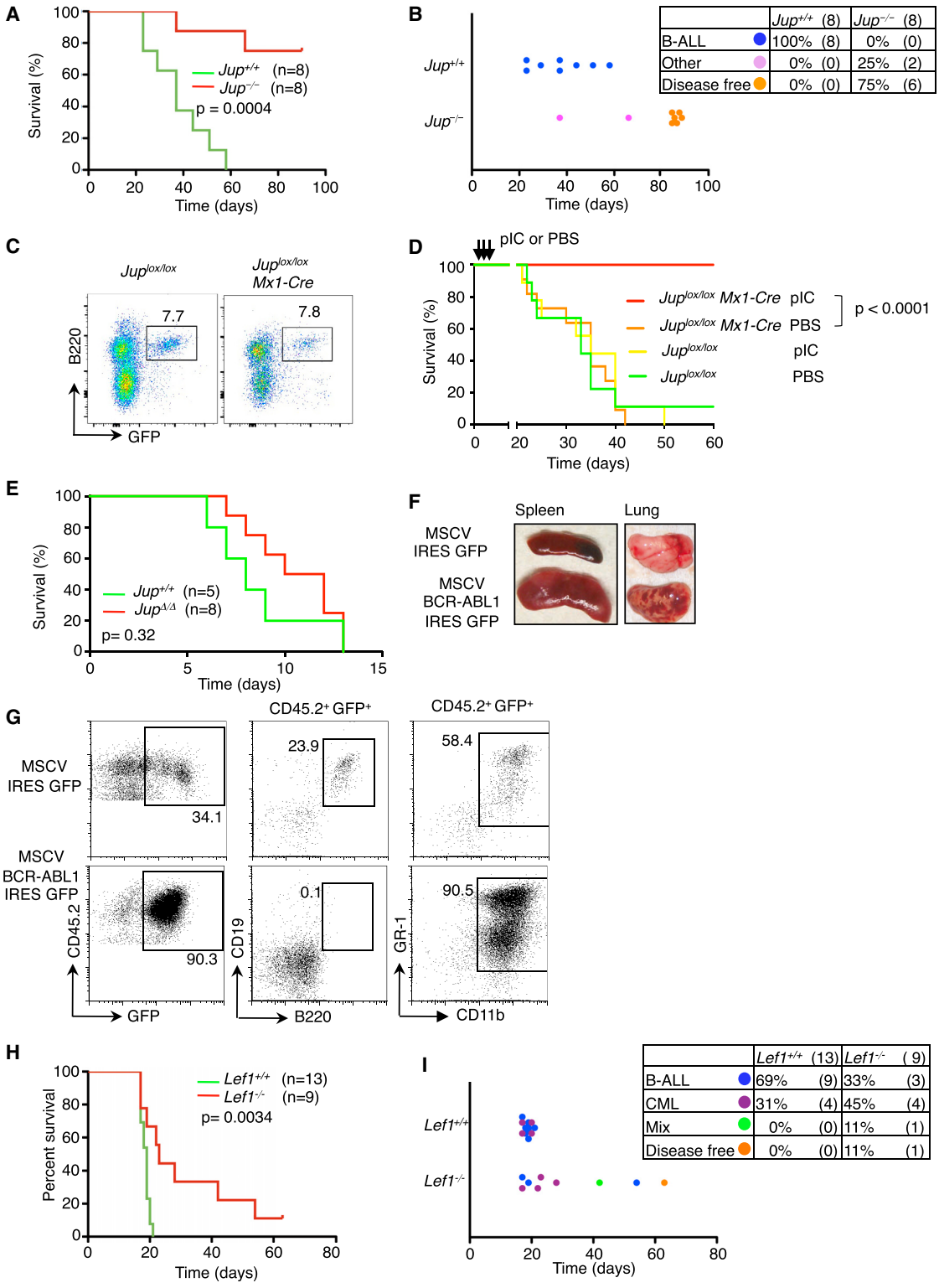

Figure 2. γ-Catenin Maintains Established Ph+ B-ALL

(A and B) WT recipients (CD45.1) were transplanted with purified B220+ CD19+ IgM− pro-B and pre-B cells transduced with BCR-ABL1 (p210), and recipient mice were analyzed for survival (compiled from two independent experiments) (A) and disease type (B).

(C and D) WT recipients (CD45.1) were transplanted with BCR-ABL1 (p185) (GFP) transduced BM cells from *Jup*$^{lox/lox}$ *Mx1-Cre* or *Jup*$^{lox/lox}$ mice (CD45.2), and recipient mice were analyzed for the presence of BCR-ABL1+ B cells in the BM 7 days later (C) and for survival following the injection of poly(I:C) pIC to delete *Jup* (D). Data are from n = 9–12 mice per group, compiled from two independent experiments.

(legend continued on next page)

$B220^+CD19^+IgM^-$ pro-B and pre-B cells readily induced B-ALL in recipient mice (8/8 recipients) (Figures 2A and 2B). These B-ALL cells were fully transformed, as they gave rise to leukemia in secondary recipients (data not shown). In contrast, $Jup^{-/-}$ pro-B and pre-B cells completely failed to induce B-ALL (0/8 recipients) (Figures 2A and 2B). The death of two of the recipients (pink dots) was not associated with an expansion of BCR-$ABL1^+$ cells. Indeed, immature B cells expressed *Jup* mRNA (Figure S2A). Thus initiation of BCR-$ABL1^+$ B-ALL in B-lineage-committed progenitor cells depended on γ-catenin.

Continuous γ-Catenin Expression Is Needed to Maintain Established Ph^+ B-ALL

We further addressed whether continuous γ-catenin expression was necessary to propagate B-ALL disease. To this end we combined a conditional *Jup* allele ($Jup^{lox/lox}$) with inducible Cre expression. BM cells from $Jup^{lox/lox}$ *Mx1-Cre* mice were transduced with BCR-ABL1 (p185) before transplantation into recipient mice. Transduced $B220^+$ cells were readily detected in the BM and blood of recipient mice 7 days later (Figure 2C and data not shown) when Cre expression was induced (using poly(I:C) [pIC] administration) to delete *Jup*. While recipients injected with pIC remained symptom free for >60 days (Figure 2D) and showed no evidence of residual disease upon sacrifice (Figure S2B), untreated recipients essentially all succumbed to B-ALL disease within 20–40 days post transplantation (Figure 2D). Recipients of $Jup^{lox/lox}$ BM (lacking *Mx1-Cre*) succumbed to B-ALL independent of pIC administration. Thus, continuous γ-catenin expression was essential to maintain B-ALL disease.

γ-Catenin and β-Catenin Play Selective Roles for B-ALL and CML, Respectively

We next determined whether γ-catenin also played a role for the development of CML-like disease. Since CML originates from HSC, we transduced purified Lin^- $Sca1^+$ $c\text{-}Kit^+$ (LSK) cells from $Jup^{lox/lox}$ and $Jup^{lox/lox}$ *Vav-Cre* ($Jup^{\Delta/\Delta}$) mice with BCR-ABL1 (p210) (Figure S2C). All recipients of control and $Jup^{\Delta/\Delta}$ LSK cells developed CML-like disease (Figures 2E and S2D), which was characterized by weight loss, splenomegaly, pulmonary hemorrhage, and aberrant expansion of $CD11b^+$ $GR1^+$ granulocytes in the BM, spleen, and blood (Figures 2F and 2G; and data not shown). CML initiation was also comparable using BM progenitors from 5-fluorouracil-treated $Jup^{+/+}$ and $Jup^{-/-}$ fetal liver chimeras (data not shown). Thus, γ-catenin was dispensable for CML but essential for the induction and maintenance of B-ALL.

Our findings together with published data (Hu et al., 2009; Zhao et al., 2007) raised the question of whether γ-catenin and β-catenin played selective roles in B-ALL and CML, respectively. While CML did not develop in the absence of β-catenin (Hu et al., 2009; Zhao et al., 2007), the majority of recipients of $Ctnnb1^{-/-}$ HSC eventually succumbed to B-ALL (Zhao et al., 2007), suggesting that β-catenin was not required for B-ALL initiation. However, since recipients of WT HSC developed CML, it was possible that β-catenin suppressed B-ALL initiation. Transduction of WT ($Ctnnb1^{lox/lox}$ or *Vav-Cre* transgenic) or $Ctnnb1^{lox/lox}$ *Vav-cre* ($Ctnnb1^{\Delta/\Delta}$) BM with BCR-ABL1 (p210) resulted in comparable B-ALL induction (8/9, 89% for WT and 8/11, 73% for $Ctnnb1^{\Delta/\Delta}$) (Figures S2E and S2F). PCR analyses confirmed *Ctnnb1* deletion in these B-ALL samples (Figure S2G). Thus β-catenin had no major role in Ph^+ B-ALL initiation, suggesting that γ-catenin and β-catenin played selective roles in B-ALL and CML, respectively.

We further addressed whether γ-catenin signaling played a role for B-ALL initiation. γ-Catenin can associate with Tcf/Lef transcription factors and transduce canonical Wnt signals (Jeannet et al., 2010). *Lef1* was the most highly expressed Tcf/Lef family member in normal (data not shown) and Ph^+ B cells in pre-leukemic mice (Figure S3A). To address a role of Lef1, we used fetal liver cells from $Lef1^{+/+}$ and $Lef1^{-/-}$ embryos (Figure S3B), which had a comparable compartment of $B220^+$ B cells (Figure S3C), except that $Lef1^{-/-}$ $B220^+$ cells lacked BP-1 (data not shown) as noted before (Reya et al., 2000). Three weeks post transplantation of BCR-ABL1 (p210) transduced fetal liver cells, recipients of $Lef1^{+/+}$ and $Lef1^{-/-}$ BM contained comparable populations of BCR-$ABL1^+$ B cells in the blood (Figure S3D), indicating equivalent engraftment and initial expansion of Ph^+ cells. However, while $Lef1^{+/+}$ fetal liver yielded B-ALL in the majority of recipients (9/13; 69%), fewer recipients of $Lef1^{-/-}$ fetal liver developed B-ALL (3/9; 33%) (Figures 2H and 2I). In contrast to Lef1, Tcf1 (encoded by the *Tcf7 gene*) did not alter B-ALL induction (Figures S3E and S3F). Thus, Lef1 played a significant role for the induction of Ph^+ B-ALL, consistent with the idea that γ-catenin acted at least in part via Lef1, and thus in the context of the canonical Wnt signaling pathway.

γ-Catenin Expression Maintains Human Ph^+ B-ALL

We next addressed whether γ-catenin was essential for human Ph^+ B-ALL. Similar to murine Ph^+ B-ALL (Figure 3A), γ-catenin protein was readily detected in six human Ph^+ cell lines (Sup-B15, K562, BV-173, TOM-1, SD-1, and NALM-1) (Figure 3B) and in patient-derived B-ALL samples (Figure 3C) as noted before (Gang et al., 2014). Knockdown of γ-catenin increased the apoptosis and suppressed the expansion of all six Ph^+ cell lines (Figures 3D, 3E, 3F, S4A, and S4B). Thus, several Ph^+ cell lines, which are resistant to the tyrosine kinase inhibitor imatinib (Sup-B15, SD-1, and NALM-1) (see later), depended on γ-catenin.

γ-Catenin knockdown also impaired the expansion of Sup-B15 cells transplanted into immunodeficient NOD $Prkdc^{scid}$ $Il2rg^{-/-}$ (NSG) mice (Figure 3G). Furthermore, patient-derived Ph^+ B-ALL cells were transduced with Sh JUP or Sh scr constructs co-expressing fluorescent proteins, which had been

(E–G) WT recipients (CD45.1) were transplanted with BCR-ABL1 (p210) transduced with Lin^- $Sca\text{-}1^+$ $c\text{-}kit^+$ (LSK) cells from $Jup^{lox/lox}$ *Vav-Cre* ($Jup^{\Delta/\Delta}$) and $Jup^{lox/lox}$ mice, and recipient mice were analyzed for survival (E), the appearance of the spleen and the lung (F), and the presence of donor-derived ($CD45.2^+$) GFP^+ (BCR-$ABL1^+$) $CD11b^+$ $Gr\text{-}1^+$ granulocytes (G).

(H and I) WT recipients (CD45.1) were transplanted with BCR-ABL1 (p210) transduced with fetal liver cells from E14 $Lef1^{+/+}$ and $Lef1^{-/-}$ embryos (CD45.2), and recipient mice were analyzed for survival (compiled from three independent experiments using n = 5–6 independent donor embryos of each type) (H) and disease type (I).

See also Figures S2 and S3.

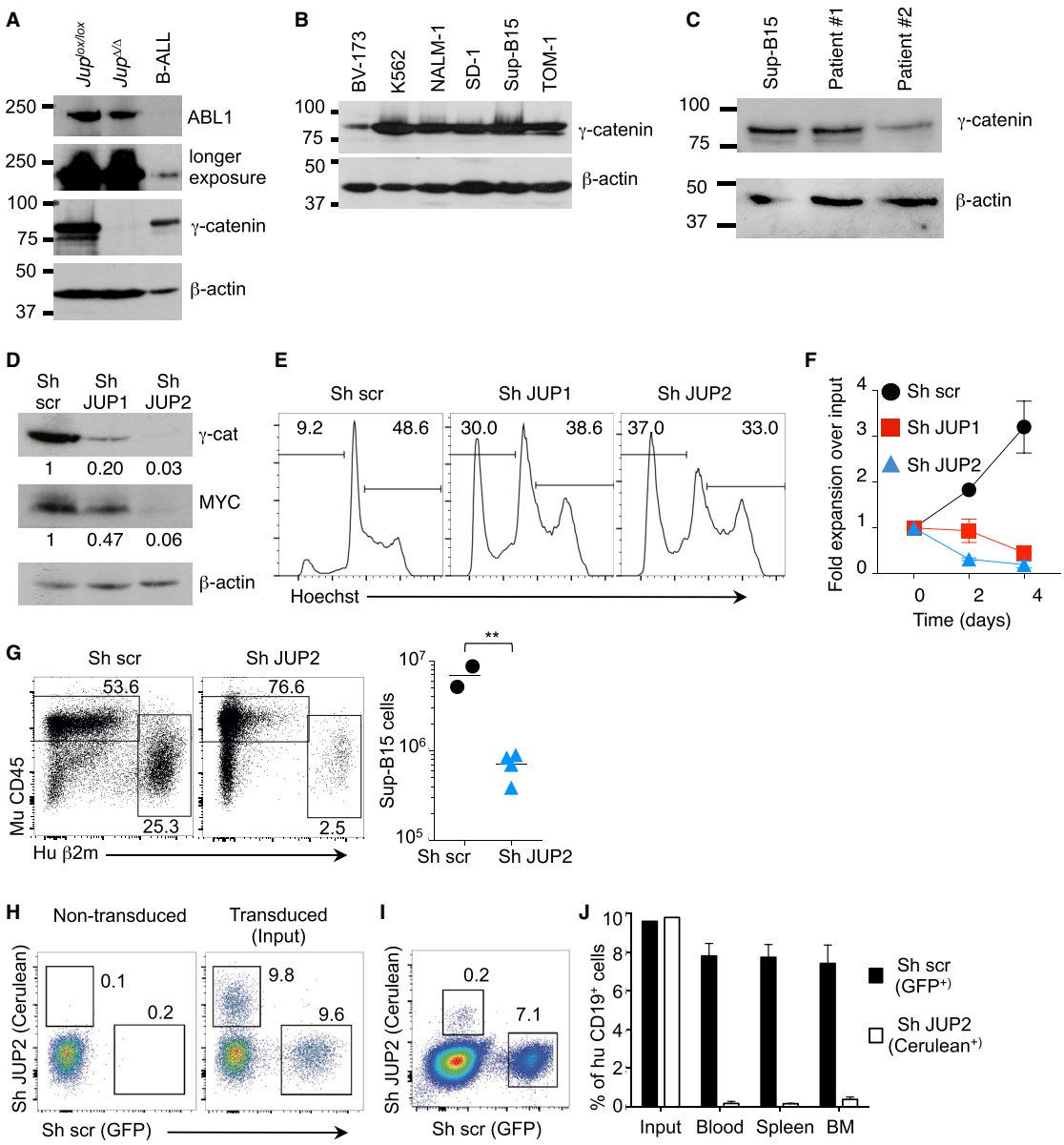

Figure 3. γ-Catenin Maintains Human Ph⁺ B-ALL

(A–C) Expression of γ-catenin in murine BCR-ABL1⁺ (p185) B cells from replating assays or primary B-ALL (A), human Ph⁺ cell lines (B), or patient-derived Ph⁺ B-ALL samples (huCD19⁺) (C).

(D–G) Sup-B15 cells stably expressing short hairpins (Sh) to γ-catenin (Sh JUP1 or Sh JUP2) or a scrambled control hairpin (Sh scr) were analyzed for the expression of γ-catenin and MYC (D), apoptosis (E), cellular expansion *in vitro* (mean number of live cells over time as compared with input) (F), or the expansion in NSG mice (G). The scatterplot shows the number of human cells (human β2m⁺) in the BM of NSG mice. All data are representative of two or more independent experiments.

(H–J) Ph⁺ B-ALL cells from patient #1 transduced with control Sh scr (GFP) and Sh JUP2 (co-expressing the cyan fluorescent protein Cerulean) constructs were analyzed for the transduction efficiency *in vitro* (input) (H) or transplanted into NSG mice and analyzed for the presence of human (hu) CD19⁺ cells expressing Sh scr (GFP⁺) or Sh JUP2 (Cerulean⁺) in the blood of recipient mice 6 weeks later (I) whereby the frequencies of transduced huCD19⁺ cells in recipient mice were compared with input (J). Representative of two experiments each with n = 3–4 mice per group.

Data in (F) and (J) are means ± SD; the horizontal bar in (G) depicts the mean. **p < 0.01. See also Figure S4.

validated in K562 cells (Figure S4C). Transduced cells were mixed in equal proportions and maintained *in vitro* for 2–6 days to verify the input (Figures 3H and S4D) or were transplanted into NSG mice. Cells expressing the control Sh scr construct (GFP⁺) represented a stable fraction of patient-derived B-ALL cells *in vivo*, and that fraction corresponded to the input. In contrast, relative to input, Sh JUP2-expressing cells (Cerulean⁺) had almost completely disappeared from peripheral blood, the spleen, and the BM of NSG mice (Figures 3I and 3J). Corresponding data were obtained using B-ALL cells from a second

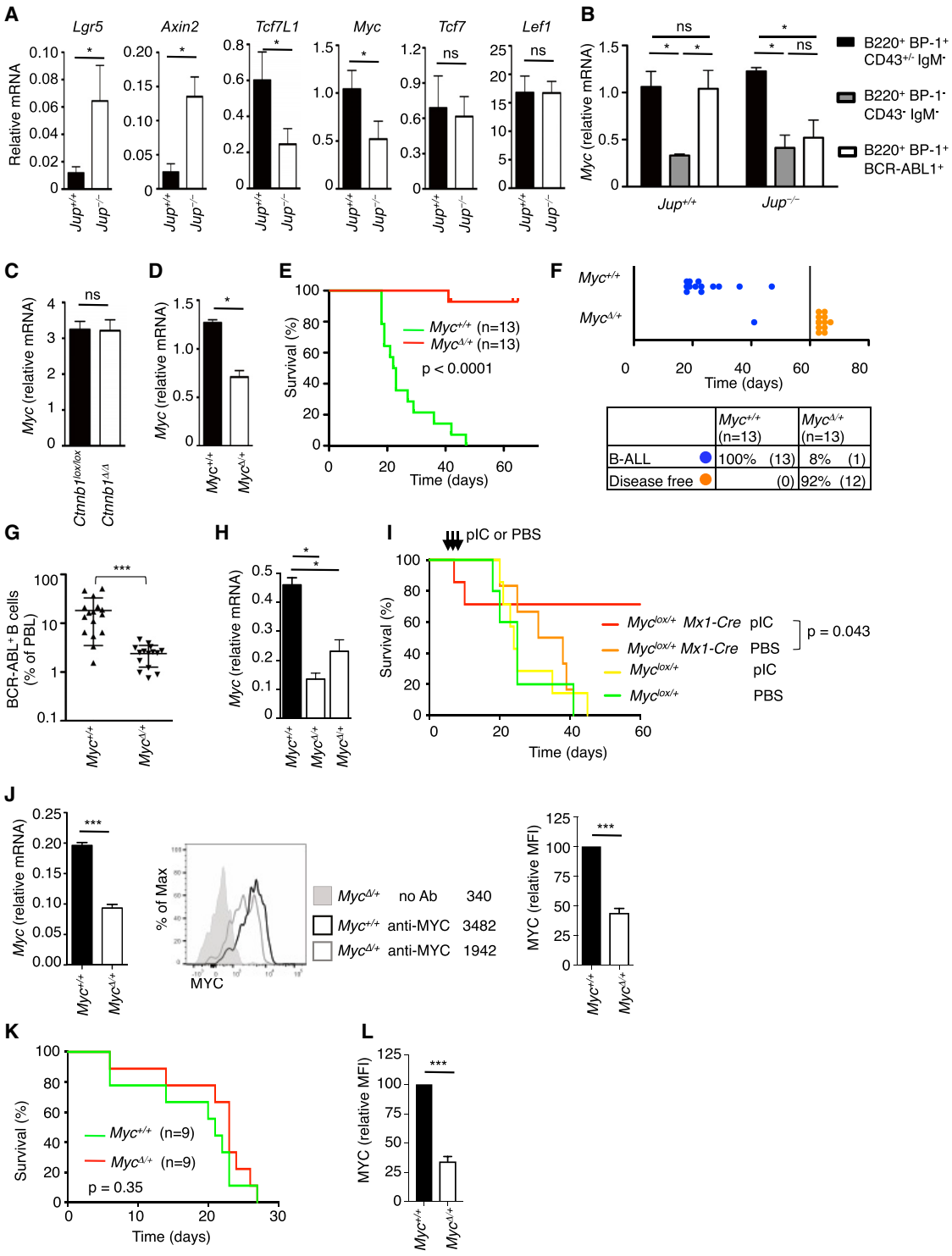

Figure 4. A Normal *Myc* Gene Dosage Is Essential to Maintain Established Ph$^+$ B-ALL

(A) Expression of the indicated Wnt target and/or pathway genes in *Jup*$^{+/+}$ and *Jup*$^{-/-}$ pre-leukemic Ph$^+$ B cells.

(B–D) Expression of *Myc* in pre-leukemic Ph$^+$ B cells compared with the corresponding and the subsequent normal stages of B cell developmental (B), in pre-leukemic *Ctnnb1*$^{lox/lox}$ and *Ctnnb1*$^{\Delta/\Delta}$ Ph$^+$ B cells (C), and in normal BP-1$^+$ pre-B cells from *Myc*$^{\Delta/+}$ as compared with *Myc*$^{+/+}$ mice (D).

(E–H) WT recipients (CD45.1) transplanted with BCR-ABL1 (p210) transduced *Myc*$^{+/+}$ or *Myc*$^{\Delta/+}$ BM were analyzed for survival (compiled from three independent experiments using n = 4–6 donors of each type) (E), disease type (F), the presence of CD45.2$^+$ BCR-ABL1$^+$ (mCherry$^+$) Ph$^+$ B cells in the blood of pre-leukemic mice (G), and *Myc* expression in pre-leukemic B cells (H).

(legend continued on next page)

patient (Figures S4D and S4E). Loss of patient-derived Ph$^+$ B-ALL cells was confirmed using a Sh JUP1 (GFP) construct versus a Sh scr [Cerulean] control (data not shown). The latter also ensured that cell loss was independent of the color combination. Collectively these data demonstrated that the maintenance of patient-derived Ph$^+$ B-ALL in xenografts depended on γ-catenin expression.

In addition to Ph$^+$ B-ALL, γ-catenin was expressed in a small set of B-ALL cell lines with distinct translocation products (Figure S4F), and the expansion of these cells also depended on γ-catenin (Figure S4G), although some of these B-ALL subtypes may also depend on β-catenin (Gang et al., 2014). Indeed *JUP* was upregulated in clinical B-ALL samples irrespective of the t(9; 22) translocation. Moreover, *JUP* was also overexpressed in certain AML subtypes, in agreement with previous studies (Morgan et al., 2012; Muller-Tidow et al., 2004; Zheng et al., 2004), but not in CML, T-ALL, or CLL (Figure S4H). In contrast, *CTNNB1* expression did not vary among hematological malignancies (Figure S4I), indicating that γ-catenin may play a role in additional hematological malignancies.

A Critical Role of the *Myc* Gene Dosage in the Maintenance of Ph$^+$ B-ALL

To identify γ-catenin target genes, we conducted a gene expression analysis of flow sorted BCR-ABL1$^+$ B220$^+$ BP-1$^+$ cells from the BM of pre-leukemic mice. This analysis identified 91 genes that were differentially expressed (adjusted p value <0.1), whereby 40 genes were upregulated and 51 were downregulated (shown in part in Table S1). Pathway analysis using GeneGO revealed an increase of "transcription regulation of granulocyte development" in the absence of γ-catenin (*Mpo*, *Elane*, and *Prtn3*, p = 0.0004). Furthermore, the top three genes expressed in granulocyte monocyte progenitors as compared with normal pre-B cells (*Elane*, *Prtn3*, and *Ctsg*) (www.immgen.org/index_content.html) were upregulated in Ph$^+$ B cells lacking γ-catenin (Table S1), suggesting that γ-catenin suppresses a myeloid gene expression program in BCR-ABL1$^+$ B cells. However, the analysis of myeloid cell-surface markers or Mpo protein did so far not provide evidence for enhanced myeloid differentiation of *Jup*$^{-/-}$ Ph$^+$ B cells (data not shown).

We next focused on the expression of Wnt pathway components and targets (http://www.stanford.edu/group/nusselab/cgi-bin/wnt/). Based on our gene array and qPCR, we identified several Wnt responsive/pathway genes whose expression was significantly decreased (*Myc*, *Tcf7L1* [Tcf3], *Grb10*), increased (*Axin2*, *CD44*, *Lgr5*) or unaltered (*Tcf7* [Tcf1], *Lef1*) in *Jup*$^{-/-}$ Ph$^+$ B cells (Figure 4A and Table S1). Thus, γ-catenin exerted diverse effects on the expression of a subset of known Wnt responsive/pathway genes.

We focused on the well-known Wnt target *Myc*, whose expression was reduced in BCR-ABL1$^+$ *Jup*$^{-/-}$ B cells based on array and qPCR analysis (2-fold, p <0.03) (Figure 4B). Compared with normal pre-B cells, BCR-ABL1 did upregulate *Myc* expression or rather, BCR-ABL1 prevented the downregulation of *Myc*, which was observed when immature B cells differentiated past the B220$^+$BP-1$^+$CD43$^{+/-}$ immunoglobulin M (IgM)$^-$ stage (Figure 4B), i.e. the passage of the pre-B cell receptor checkpoint. Thus, BCR-ABL1 sustained *Myc* expression and this was reduced approximately 50% in the absence of γ-catenin. In the absence of β-catenin, *Myc* expression was not altered (Figure 4C).

We hypothesized that the 2-fold reduction in *Myc* expression was critical for B-ALL initiation or maintenance. To mimic this situation, we exploited *Myc* heterozygous mice (*Myc*$^{lox/+}$ × *Vav-Cre* termed *Myc*$^{\Delta/+}$) (Figure S5A). Deletion of a single *Myc* allele indeed reduced *Myc* mRNA in pre-B cells by approximately 50% (Figure 4D) but had no significant effect on B cell development (Figure S5B). Transduction of *Myc*$^{+/+}$ control BM with BCR-ABL1 (p210) mediated B-ALL disease in 100% of recipient mice (13/13; 100%). In contrast, a single recipient of *Myc*$^{\Delta/+}$ BM developed B-ALL disease (1/13, 8%) and most recipients remained disease free for >60 days post transplantation (Figures 4E and 4F). Thus, a reduced *Myc* gene dosage prevents B-ALL induction.

While *Myc*$^{+/+}$ and *Myc*$^{\Delta/+}$ BM cells were transduced with comparable efficiencies (data not shown), there were fewer pre-leukemic *Myc*$^{\Delta/+}$ B cells (Figure 4G) and these expressed >50% less *Myc* mRNA compared with corresponding *Myc*$^{+/+}$ cells (Figure 4H). While BCR-ABL1$^+$ *Myc*$^{\Delta/+}$ B cells eventually vanished, non-transduced (mCherry$^-$) *Myc*$^{\Delta/+}$ LSK cells (CD45.2$^+$) remained present and these contributed long-term to all hematopoietic lineages including B cells (Figure S5C and data not shown). Unlike B-ALL initiation, normal B cell development was thus not *Myc* dosage sensitive. We further addressed whether the continuous presence of both *Myc* alleles was needed to maintain Ph$^+$ B-ALL. To this end, we transduced *Myc*$^{lox/+}$ *Mx1-Cre* BM with BCR-ABL1 (p185) before transplantation into recipient mice. Seven days post transplantation, deletion of one *Myc* allele was induced by pIC treatment. The majority of pIC-treated animals survived >60 days while untreated recipients succumbed to B-ALL disease between days 40 and 45 post transplantation (Figure 4I). Recipients of *Myc*$^{lox/+}$ BM (lacking *Mx1-Cre*) succumbed to B-ALL independent of pIC treatment (Figure 4I). Thus, the maintenance of Ph$^+$ B-ALL depends on the continuous presence of both *Myc* alleles.

While *Myc* is required for CML initiation, we addressed whether CML initiation was *Myc* gene dosage dependent. Compared with *Myc*$^{+/+}$, *Myc*$^{\Delta/+}$ LSK cells indeed expressed around 50% less *Myc* mRNA or protein (Figure 4J). Following transduction with BCR-ABL1 and transplantation, *Myc*$^{+/+}$ and *Myc*$^{\Delta/+}$ LSK cells yielded CML with equivalent efficiency (Figure 4K) in agreement with Reavie et al. (2013). PCR analyses ensured that *Myc*$^{\Delta/+}$ CML were indeed devoid of one *Myc* allele (Figure S5D), and flow cytometry showed that BCR-ABL1$^+$ *Myc*$^{\Delta/+}$ LSK cells

(I) WT recipients (CD45.1) transplanted with BCR-ABL1 (p185) (GFP) transduced *Myc*$^{lox/+}$ and *Myc*$^{lox/+}$ *Mx1-Cre* BM cells (CD45.2) were injected with pIC beginning 7 days later and analyzed for survival. Data are from one experiment with n = 5–7 mice per group.
(J) LSK cells from *Myc*$^{+/+}$ and *Myc*$^{\Delta/+}$ mice were analyzed for MYC expression using qRT-PCR and flow cytometry. Numbers indicate the MFI of MYC staining.
(K) Survival of WT recipients (CD45.1) transplanted with BCR-ABL1 (p210) transduced *Myc*$^{+/+}$ and *Myc*$^{\Delta/+}$ LSK cells.
(L) MYC expression in *ex vivo* isolated BCR-ABL1$^+$ (p210) *Myc*$^{+/+}$ and *Myc*$^{\Delta/+}$ LSK cells.
All bar graphs and the scatterplot (G) show means ± SD. *p < 0.05, **p < 0.01, p < 0.001. ns, not significant (p > 0.05). See also Figure S5 and Table S1.

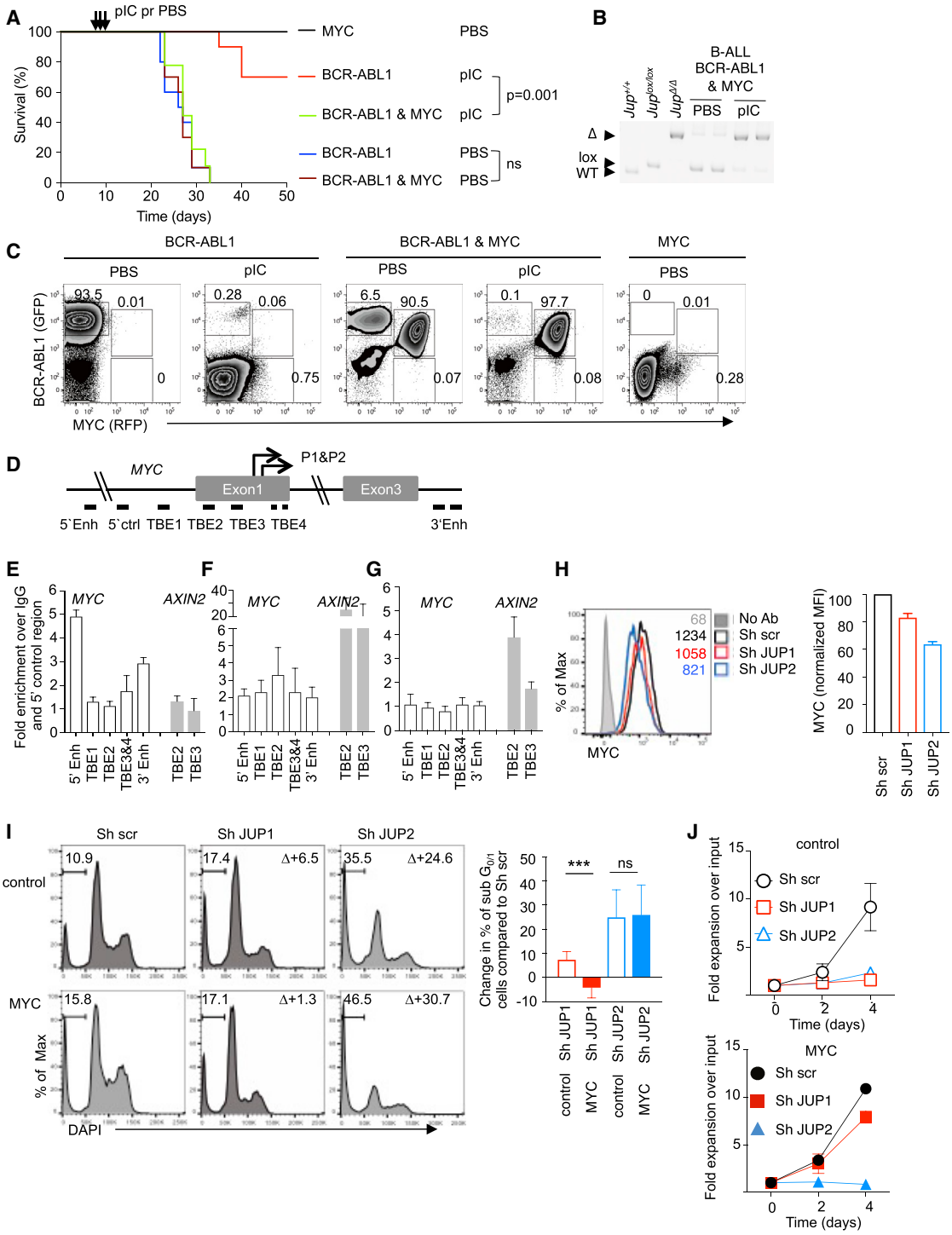

Figure 5. MYC Is an Essential γ-Catenin Target in Ph$^+$ B-ALL

(A) Survival of WT recipients (CD45.1) transplanted with MYC (RFP) and/or BCR-ABL1 (p185) (GFP) transduced *Jup$^{lox/lox}$ Mx1-Cre* BM cells (CD45.2) and treated with pIC (beginning on day 7). Data are from two independent experiments with n = 9–10 per group, except n = 4 mice for the MYC-only group.

(B) PCR analyses to confirm *Jup* deletion in sorted B-ALL cells of the indicated type.

(C) BCR-ABL1 (GFP) and MYC (RFP) expression by CD45.2$^+$ B220$^+$ cells from the indicated type of diseased recipients or from symptom-free recipients that were sacrificed >50 days after transplantation (i.e., recipients of BCR-ABL1/pIC or MYC BM).

(D) Schematic representation of Tcf/Lef-binding element sites (TBE) in the promoter (P1 and P2) and in 5′ and 3′ enhancer (Enh) elements of the human *MYC* locus.

(E–G) ChIP for γ-catenin (E), LEF1 (F), and β-catenin (G) using Sup-B15 chromatin followed by qPCR for indicated TBE in the *MYC* or in the control *AXIN2* locus. Bars depict mean fold enrichment relative to a control (ctrl) region in the same locus and relative to IgG isotype control ChIP. Data are compiled from three independent determinations.

(legend continued on next page)

expressed around 50% less MYC protein than WT (Figure 4L). Unlike B-ALL, CML initiation was thus not *Myc* gene dosage sensitive. The selective role of γ-catenin in B-ALL can thus be explained by the 50% reduction of MYC expression in the absence of γ-catenin.

MYC Is an Essential and Direct γ-Catenin Target in Ph$^+$ B-ALL

To address whether MYC was an essential γ-catenin target, we determined whether ectopic MYC maintained murine Ph$^+$ B-ALL when *Jup* was deleted. BM cells from *Jup$^{lox/lox}$ Mx1-Cre* mice were transduced with MYC (RFP$^+$) and/or BCR-ABL1 (p185) (GFP$^+$) before transplantation into recipient mice. Seven days later, when the recipient's BM harbored a population of GFP$^+$ B220$^+$ B cells (data not shown), *Jup* was deleted via pIC treatment. Recipients of BCR-ABL1 BM succumbed to B-ALL when left untreated, but survived for >50 days when treated with pIC (Figure 5A) as also shown in Figure 2D. Conversely, recipients of BCR-ABL1 and MYC BM all succumbed to B-ALL despite pIC treatment (Figure 5A). PCR analyses confirmed that the *Jup* locus had been deleted (Figure 5B) and flow cytometry showed that BCR-ABL1 and MYC were co-expressed (Figure 5C). Of note, recipients of BM only transduced with MYC remained healthy (Figure 5A) and B cells expressing ectopic MYC were only observed when co-expressing BCR-ABL1 (Figure 5C). Thus, MYC expression was sufficient to maintain murine Ph$^+$ B-ALL in the absence of γ-catenin.

We next used chromatin immunoprecipitation (ChIP) to determine whether γ-catenin occupied Tcf/Lef consensus-binding elements in the *MYC* locus of human Ph$^+$ cell lines (Figure 5D). Significant γ-catenin occupancy was detected at 5′ as well as 3′ *MYC* enhancer elements but not at the *MYC* promoter or the control *AXIN2* locus (Figures 5E, S6A, and S6B). Furthermore, LEF1 was also bound to the 5′ and the 3′ *MYC* enhancer elements as well as to the *MYC* promoter and the *AXIN2* locus (Figure 5F). In contrast, β-catenin occupied the *AXIN2* locus and was not associated with the *MYC* locus (Figure 5G). Indeed, knockdown of β-catenin did not alter *MYC* expression in Ph$^+$ cell lines (Figure S6C). Thus, *MYC* was a direct γ-catenin target in Ph$^+$ cells.

Knockdown of γ-catenin in human Ph$^+$ cells reduced MYC expression (Figures 3D, S4A, and 5H), increased the expression of the MYC target p21 (*CDKN1A*) (Figure S6D), and decreased cellular survival and expansion (Figures 3E, 3F, S4A, 5I, and 5J). The latter effects were reproduced by MYC knockdown (Figure S6E). Ectopic MYC improved the survival and restored cellular expansion when γ-catenin knockdown was moderate using Sh JUP1, but not when γ-catenin knockdown was more complete using Sh JUP2 (Figures 5I and 5J). The expression of γ-catenin constructs, which were resistant to Sh JUP1 or Sh JUP2, rescued cellular expansion (Figure 7D and data not shown), demonstrating that γ-catenin was the essential target of both Sh constructs. Thus, additional γ-catenin targets seemed to contribute to the survival of human Ph$^+$ cells.

BIRC5 Is an Additional γ-Catenin Target in Ph$^+$ B-ALL

Screening Ph$^+$ cells for γ-catenin-dependent pro-survival factors uncovered reduced BIRC5 (Survivin) expression upon γ-catenin knockdown (Figure 6A), in agreement with Niu et al. (2013). γ-Catenin reportedly associates with and promotes the activity of the *BIRC5* promoter (Kim et al., 2011), and BIRC5 knockdown reduced the viability of a Ph$^+$ B-ALL cell line (Tyner et al., 2012). The relevance of BIRC5 as γ-catenin target was addressed by ectopic BIRC5 expression. Ectopic BIRC5 restored the expansion of Ph$^+$ cells using either Sh JUP1 or Sh JUP2 for γ-catenin knockdown (Figure 6B). These data thus identified BIRC5 as an additional functionally relevant γ-catenin target in human Ph$^+$ cells. BIRC5 is also regulated by MYC in Ph$^+$ cells (Fang et al., 2009) and its promoter was bound by MYC (Figure S6F). Indeed, ectopic MYC was sufficient to restore BIRC5 expression upon γ-catenin knockdown using Sh JUP1 (Figure 6C). Thus, *BIRC5* was also an MYC target and consequently both an indirect as well as a direct γ-catenin target.

We extended the above analyses to murine Ph$^+$ B-ALL. Compared with WT B-ALL, BIRC5 expression was reduced when γ-catenin was deleted. Conversely, BIRC5 was increased when WT B-ALL expressed MYC (Figure 6D), indicating that BIRC5 was also regulated by γ-catenin and MYC in murine Ph$^+$ B-ALL. To address the relevance of BIRC5, we ectopically expressed human BIRC5 in primary murine B-ALL followed by *Jup* deletion *in vivo*, as shown above (Figures 2D and 5A). Recipients of BCR-ABL1 or BCR-ABL1 and BIRC5 BM all succumbed to B-ALL disease (Figure 6E). When mice were treated with pIC to delete *Jup* a single recipient of BCR-ABL1 BM developed B-ALL (1/10), in agreement with Figures 2D and 5A. In contrast, most recipients of BCR-ABL1 and BIRC5 BM succumbed to B-ALL despite pIC treatment (Figure 6E). We confirmed that these latter B-ALL had a deleted *Jup* locus (Figure 6F) and expressed the transduced *BIRC5* (Figure 6G). Of note, recipients of BM only transduced with BIRC5 remained disease free (>60 days) (Figure 6E). Thus, ectopic BIRC5 was sufficient to maintain Ph$^+$ B-ALL *in vivo* following γ-catenin ablation, indicating that also BIRC5 was a functionally relevant γ-catenin target in Ph$^+$ B-ALL.

Tyrosine Residues in γ-Catenin Are Essential for Ph$^+$ Cell Expansion and γ-Catenin Recruitment to the *MYC* Locus

Finally we addressed how BCR-ABL1 regulated γ-catenin to maintain B-ALL. Compared with the normal stage of B cell development, BCR-ABL1 expression did not affect *Jup* mRNA expression (Figure 7A), indicating that γ-catenin was not regulated by transcriptional mechanisms. In CML, BCR-ABL1 stabilizes β-catenin through tyrosine phosphorylation (Coluccia et al., 2007). In contrast, γ-catenin protein amounts did not differ between murine B cell colonies induced by interleukin-7 (IL-7) or BCR-ABL1 (Figure S7A) or when transfecting γ-catenin with or without BCR-ABL1 into 293T cells (Figure S7B), indicating

(H–J) Human Ph$^+$ cells (Sup-B15) stably expressing GFP (control) or MYC were transduced with Sh scr, Sh JUP1, and Sh JUP2 constructs and analyzed for MYC expression (normalized mean fluorescence intensity [MFI] of n = 3 independent experiments) (H), the abundance of apoptotic cells (change in the percentage of dead cells compared with the corresponding Sh scr control [n = 8, from four independent experiments]) (I), and cellular expansion (n = 3 determinations per time point, representative of >5 experiments) (J).

Error bars in (E) to (J) represent SD. ***p < 0.01. ns, not significant (p > 0.05). See also Figure S6.

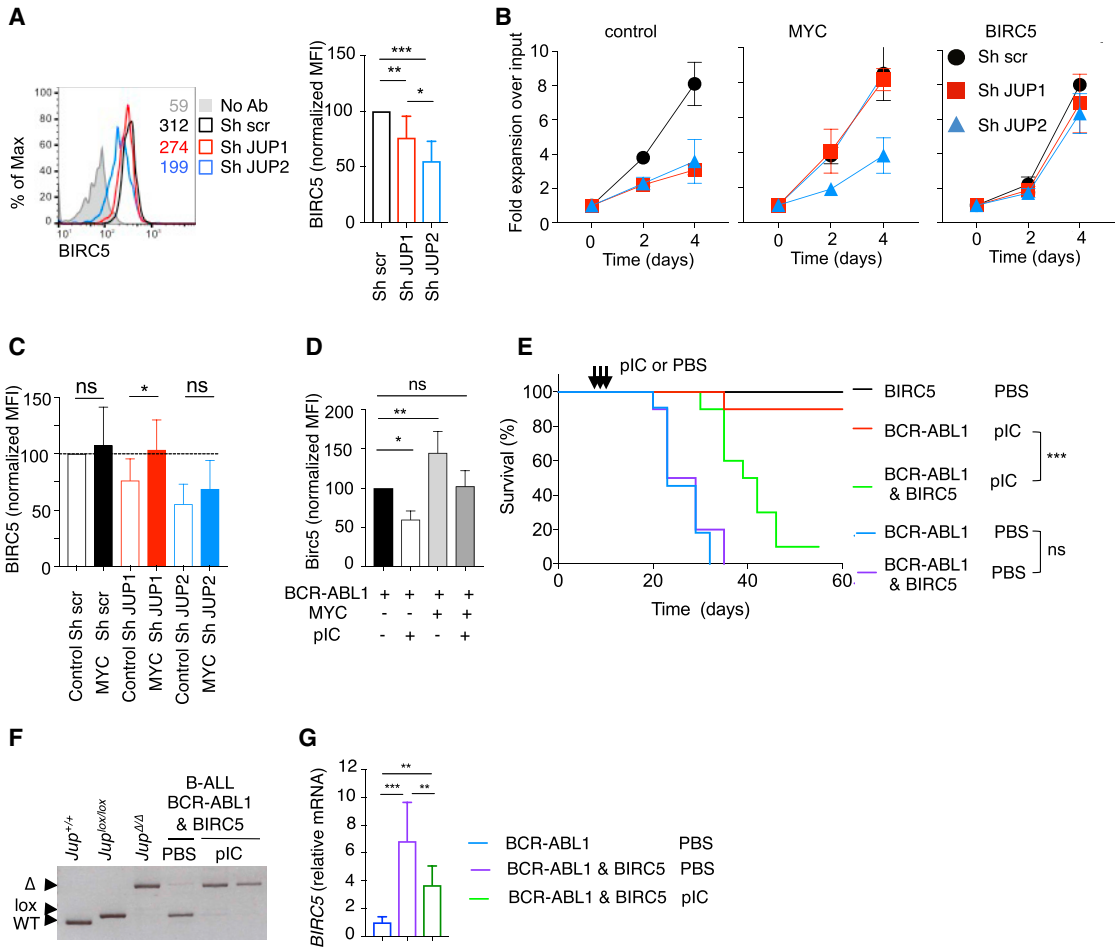

Figure 6. BIRC5 Is an Essential γ-Catenin Target in B-ALL

(A and B) Ph$^+$ cells (K562) expressing GFP (control), MYC or BIRC5 were stably transduced with control Sh scr, Sh JUP1, or Sh JUP2 constructs and analyzed for BIRC5 expression (normalized MFI of staining, >6 determinations) (A) and cellular expansion (n = 3 determinations per time point, representative of n = 3 independent experiments) (B).

(C) BIRC5 expression (normalized MFI) in MYC-expressing human Ph$^+$ cells following γ-catenin knockdown form n = 6–11 determinations.

(D) BIRC5 expression (normalized MFI) in primary murine B-ALL samples. n = 4 determinations derived from three independent samples.

(E) Survival of WT recipients (CD45.1) that were transplanted with BIRC5 and/or BCR-ABL1 (p185) (Cherry) transduced *Jup*$^{lox/lox}$ *Mx1-Cre* BM cells (CD45.2) and treated with pIC or PBS (beginning on day 7). Data are from n = 9–10 mice per group compiled from two independent experiments.

(F) PCR analyses to confirm *Jup* deletion in sorted CD45.2$^+$ B220$^+$ B-ALL cells of the indicated type.

(G) qRT-PCR analysis to confirm *BIRC5* expression in BIRC5 transduced B-ALL cells.

Error bars in (A) to (D) and (G) represent SD. *p < 0.05, **p < 0.01, ***p < 0.001. ns, not significant (p > 0.05).

that BCR-ABL1 did not stabilize γ-catenin protein. Notwithstanding, γ-catenin was tyrosine phosphorylated upon co-transfection with kinase-active, but not with kinase-dead BCR-ABL1 in 293T cells (Figure S7B), and endogenous (data not shown) and stably transfected γ-catenin was tyrosine phosphorylated in Sup-B15 cells (Figure 7B). We addressed the regulation of γ-catenin tyrosine phosphorylation using small-molecule inhibitors (Rix et al., 2007). The ABL and SRC family kinase inhibitor dasatinib reduced γ-catenin tyrosine phosphorylation and induced apoptosis of Sup-B15 cells, while imatinib (which inhibits ABL and a few receptor tyrosine kinases) or the ABL inhibitor nilotinib had no effect (Figures 7B and 7C). The combination of nilotinib with the SRC inhibitor SU6656, but not SU6656 alone, suppressed γ-catenin tyrosine phosphorylation (Figure 7B) and induced apoptosis (Figure 7C). The latter was similarly observed in SD-1 and NALM-1 cells (data not shown). Survival of Ph$^+$ cells and γ-catenin phosphorylation thus depended on the combined action of BCR-ABL1 and SRC family kinases.

We next addressed whether tyrosines (Y) in γ-catenin that can be phosphorylated by SRC family kinases (Miravet et al., 2003) played a role in Ph$^+$ B-ALL maintenance. To this end Y133, Y550, and Y644 of γ-catenin were mutated to phenylalanine (F). The triple Y133F, Y550F, Y644F mutant γ-catenin (γ-cat Mut) and WT γ-catenin (γ-cat WT) constructs were further rendered resistant to Sh JUP1 by introducing silent point mutations before stable expression in Sup-B15 cells. Following knockdown of endogenous γ-catenin, the WT γ-catenin construct rescued cellular expansion while the triple mutant essentially failed to

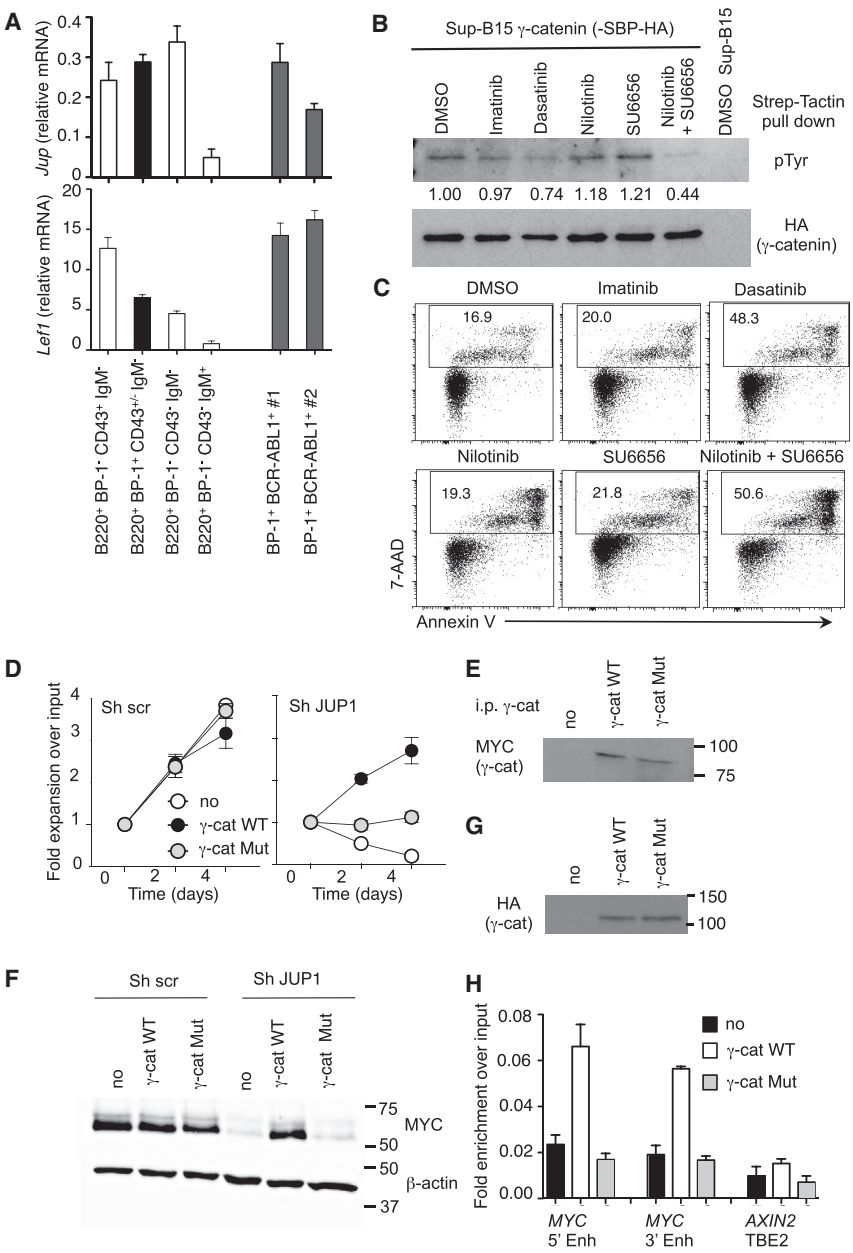

Figure 7. Tyrosine Residues in γ-Catenin Are Essential for Ph$^+$ Cell Expansion, *MYC* Expression, and γ-Catenin Recruitment to the *MYC* Locus

(A) Expression of *Jup* and *Lef1* during B cell developmental and in pre-leukemic Ph$^+$ B cell samples.

(B) Sup-B15 cells expressing HA-SBP-tagged γ-catenin were treated with imatinib, nilotinib (ABL inhibitor), dasatinib, or SU6656. γ-Catenin pull-down was analyzed for tyrosine phosphorylation.

(C) Sup-B15 cells were treated with the indicated inhibitors and apoptosis was analyzed after 24 h using flow cytometry for annexin versus 7-AAD.

(D–F) Sup-B15 cells were transduced with mCherry (control), MYC-tagged WT γ-catenin (γ-cat WT), or a γ-catenin construct in which tyrosine (Y) 133, 550, and 644 were changed to phenylalanine (F) (γ-cat Mut). In addition, silent mutations were introduced to render the constructs resistant to Sh JUP1. Following knockdown of endogenous γ-catenin, we determined cellular expansion (D), expression of the γ-catenin constructs (E), and expression of MYC (F).

(G) Expression of HA-SBP-tagged γ-cat WT and γ-cat Mut in Sup-B15 cells.

(H) ChIP for HA followed by qPCR for the TBE in the 5′ and 3′ enhancers of the *MYC* locus or for TBE2 present in the *AXIN2* locus. Data are mean fold enrichment relative to input of triplicate determinations, representative of two independent experiments.

Error bars in (A), (D), and (H) represent SD.

See also Figure S7.

Conversely, β-catenin played no essential role in B-ALL progression but has previously been shown to be essential for CML (Hu et al., 2009; Zhao et al., 2007). These data identified unanticipated, non-redundant roles of γ-catenin and β-catenin for the emergence of lymphoid and myeloid leukemia, respectively. The key role of γ-catenin in B-ALL progression was explained by a reduced expression of *Myc* and *Birc5* together with a critical dependence of B-ALL on a normal *Myc* gene dosage.

do so (Figure 7D). The WT and the mutant constructs were expressed at similar levels (Figure 7E), which further indicated that these tyrosine residues did not contribute to γ-catenin protein stabilization. Rather, deficient rescue by the mutant γ-catenin was associated with reduced *MYC* expression (Figure 7F). This was accounted for by the absence of the mutant γ-catenin from the *MYC* 5′ and 3′ enhancers (Figures 7G and 7H). Thus, the Y133, Y550, and Y644 residues are critical for the recruitment of γ-catenin to the *MYC* locus and for high MYC expression, which was critical for the maintenance of Ph$^+$ B-ALL.

DISCUSSION

Here we report an essential and selective role of γ-catenin for the progression of BCR-ABL1-induced B-ALL but not CML. It has been unclear whether γ-catenin plays significant roles in tumorigenesis and, if so, whether γ-catenin functions in the context of the canonical Wnt pathway. In solid tumors, γ-catenin loss correlates with tumor progression, development of metastasis, and poor clinical outcome (Aktary and Pasdar, 2012). Loss of γ-catenin is thought to enhance β-catenin signaling due to reduced competition for Lef/Tcf binding. Thus γ-catenin is thought to act as a tumor suppressor in solid cancers. On the other hand, γ-catenin is highly expressed in circulating tumor cell clusters and holds these clusters together (Aceto et al., 2014). Here it is possible that metastatic spread depends on the adhesive role of γ-catenin. Based on mouse models, human cell lines, and patient-derived samples, our data provided evidence that γ-catenin acted as a non-oncogene addiction gene in Ph$^+$ B-ALL. In addition γ-catenin may also play a role

in Ph-negative B-ALL. Indeed *JUP* is upregulated in clinical B-ALL samples independent of t(9;22) translocation as well as in AML. However, mutations in γ-catenin are rare (42 out of 7,426 samples, www.sanger.ac.uk/genetics/CGP/) and these are not associated with tumors of hematopoietic origin, indicating that γ-catenin is not an oncogene in hematological malignancies.

A key role for the signaling function of γ-catenin was supported by the finding that γ-catenin expression in Ph^+ B-ALL sustained the expression of BIRC5 and MYC, which were previously identified as prominent Wnt/β-catenin/Tcf4 targets in colorectal cancer (He et al., 1998; Kim et al., 2003). In B-ALL, key *MYC* enhancer elements were directly associated with Lef1 and γ-catenin, but not β-catenin, and γ-catenin significantly contributed to MYC expression. Direct binding of γ-catenin to the *MYC* promoter has previously been described in AML cell lines (Muller-Tidow et al., 2004) and in primary keratinocytes (Williamson et al., 2006). In the latter instance, however, γ-catenin binding was associated with *Myc* repression and cell-cycle arrest (Williamson et al., 2006). Interestingly, the Tcf/Lef site present in the 5′ *MYC* enhancer, which is 300 kb away from the promoter, affects colon cancer progression, and an SNP within this element influences the binding of Tcf4 and β-catenin (Tuupanen et al., 2009). It will thus be interesting to determine whether this SNP influences γ-catenin/Lef1 binding and the predisposition to B-ALL.

Our data suggested that B-ALL initiation and maintenance critically depended on the *Myc* gene dosage, while CML initiation was more resistant to reduced MYC expression, as shown herein and by others (Reavie et al., 2013). Since the deletion of γ-catenin reduced *Myc* expression by approximately 50%, these data explained the selective requirement of γ-catenin for B-ALL. Indeed, *Myc* expression was not significantly reduced in the absence of β-catenin, which further underlined the distinct behavior of Ph^+ B-ALL and CML and thus the lineage-selective roles of the two Wnt pathway intermediates.

B-ALL can be suppressed by the ABL and SRC family kinase inhibitor dasatinib but not with single ABL kinase inhibitors (Hu et al., 2006; Rix et al., 2007). Indeed, initiation of B-ALL depends on the activity of SRC family kinases (Hu et al., 2004) and these contribute to the resistance of B-ALL to single ABL kinase inhibition (Hu et al., 2006; Rix et al., 2007). Along the same line, the function of γ-catenin was controlled by the simultaneous action of ABL, and SRC family kinases and tyrosine residues in γ-catenin, which can be phosphorylated by SRC kinases (Miravet et al., 2003), were essential for B-ALL expansion. Indeed, B-ALL cell lines that are resistant to single ABL kinase inhibition were susceptible to γ-catenin ablation.

Targeting the canonical Wnt pathway has significant potential to improve the treatment of several types of leukemia. However, Wnt signaling is also critical for the renewal of the intestinal lining, the skin, and the hematopoietic system. Thus, blocking the Wnt/β-catenin pathway will likely have serious side effects. The role of γ-catenin as a key factor for B-ALL progression now raises the possibility to target a disease-specific component of the pathway. This may considerably reduce potential side effects and increase the therapeutic window for the treatment of B-ALL using selective inhibitors.

STAR★METHODS

Detailed methods are provided in the online version of this paper and include the following:

- KEY RESOURCES TABLE
- CONTACT FOR REAGENT AND RESOURCE SHARING
- EXPERIMENTAL MODEL AND SUBJECT DETAILS
- METHOD DETAILS
  - Mouse Strains
  - Fetal Liver Chimeras
  - Constructs, Viral Vectors, Virus Production and Stable Transfectants
  - Murine Ph^+ Leukemia
  - Flow Cytometry
  - PCR
  - Affymetrix Microarray
  - Colony Formation
  - Cell Culture and Inhibitor Treatment
  - shRNA Assays
  - Primary Human Ph^+ B-ALL Samples
  - Pull Down and Western Blots
  - Chromatin Immunoprecipitation (ChIP)
  - Data Analyses
- DATA AND SOFTWARE AVAILABILITY

SUPPLEMENTAL INFORMATION

Supplemental Information can be found online at https://doi.org/10.1016/j.ccell.2019.03.005.

ACKNOWLEDGMENTS

We are grateful to C. Soneson (SIB) for bioinformatics support, the Flow Cytometry and the Genomic Technologies facilities of the University of Lausanne for expert technical assistance, A. Wolfer (CHUV), X. Jiang (Terry Fox Laboratory, Vancouver), and A. Ochsenbein (University of Bern) for providing constructs or cells, and E. Mueller (Vetsuisse), G. Radice (Thomas Jefferson, Philadelphia), R. Grosschedl (MPI, Freiburg), H. Clevers (Hubrecht Institute, Utrecht), A. Trumpp (DKFZ, Heidelberg), and W. Birchmeier (MDC, Berlin) for providing mouse strains. This research was supported in part by a prize from the Leenaards Foundation 2006 (to J.H., Y.C., and W.H.) and a Sinergia grant from the Swiss National Science Foundation (SNSF) (to J.H. and W.H.) (CRSII3_136245). W.H. was supported by grants from the Fondation Emma Muschamp (26078333), the SNSF (310030_159598 and 310030B_179570), and the Swiss Cancer League (SCL) (KFS-3601-02-2015). J.-P.B. was supported in part by grants from the SNSF (310030-133108), the SCL (KLS-4237-08-2017), the foundation 'Kind und Krebs', the 'Krebsliga Zurich', the Sassella Foundation, the Fondation Panacée, and the clinical research focus program 'Human Hemato-Lymphatic Diseases' of the University of Zurich. M.T. acknowledges support from the SCL (KFS-4095-02-2017-R) and the SNSF (310030_166627/1).

AUTHOR CONTRIBUTIONS

N.L.-G., I.P., B.J.-R., M.C., I.S., Y.H., A.I., S.C., G.S.A., M.D., and M.J. conducted experiments. B.B., M.T., and J.-P.B. supervised experiments. G.C., O.H., and Y.C. and provided samples or reagents. J.H. and W.H. designed the experiments, supervised experiments, and wrote the paper.

DECLARATION OF INTERESTS

The authors declare no competing interests.

Received: October 30, 2015
Revised: January 29, 2019
Accepted: March 14, 2019
Published: April 15, 2019

REFERENCES

Aceto, N., Bardia, A., Miyamoto, D.T., Donaldson, M.C., Wittner, B.S., Spencer, J.A., Yu, M., Pely, A., Engstrom, A., Zhu, H., et al. (2014). Circulating tumor cell clusters are oligoclonal precursors of breast cancer metastasis. Cell *158*, 1110–1122.

Aktary, Z., and Pasdar, M. (2012). Plakoglobin: role in tumorigenesis and metastasis. Int. J. Cell Biol. *2012*, 189521.

Coluccia, A.M., Vacca, A., Dunach, M., Mologni, L., Redaelli, S., Bustos, V.H., Benati, D., Pinna, L.A., and Gambacorti-Passerini, C. (2007). Bcr-Abl stabilizes beta-catenin in chronic myeloid leukemia through its tyrosine phosphorylation. EMBO J. *26*, 1456–1466.

Fang, Z.H., Dong, C.L., Chen, Z., Zhou, B., Liu, N., Lan, H.F., Liang, L., Liao, W.B., Zhang, L., and Han, Z.C. (2009). Transcriptional regulation of survivin by c-Myc in BCR/ABL-transformed cells: implications in anti-leukaemic strategy. J. Cell Mol. Med. *13*, 2039–2052.

Feldhahn, N., Henke, N., Melchior, K., Duy, C., Soh, B.N., Klein, F., von Levetzow, G., Giebel, B., Li, A., Hofmann, W.K., et al. (2007). Activation-induced cytidine deaminase acts as a mutator in BCR-ABL1-transformed acute lymphoblastic leukemia cells. J. Exp. Med. *204*, 1157–1166.

Gang, E.J., Hsieh, Y.T., Pham, J., Zhao, Y., Nguyen, C., Huantes, S., Park, E., Naing, K., Klemm, L., Swaminathan, S., et al. (2014). Small-molecule inhibition of CBP/catenin interactions eliminates drug-resistant clones in acute lymphoblastic leukemia. Oncogene *33*, 2169–2178.

He, T.-C., Sparks, A.B., Rago, C., Hermeking, H., Zawel, L., da Costa, L.T., Morin, P.J., Vogelstein, B., and Kinzler, K.W. (1998). Identification of c-MYC as a target of the APC pathway. Science *281*, 1509–1512.

Heidel, F.H., Bullinger, L., Feng, Z., Wang, Z., Neff, T.A., Stein, L., Kalaitzidis, D., Lane, S.W., and Armstrong, S.A. (2012). Genetic and pharmacologic inhibition of beta-catenin targets imatinib-resistant leukemia stem cells in CML. Cell Stem Cell *10*, 412–424.

Hemann, M.T., Bric, A., Teruya-Feldstein, J., Herbst, A., Nilsson, J.A., Cordon-Cardo, C., Cleveland, J.L., Tansey, W.P., and Lowe, S.W. (2005). Evasion of the p53 tumour surveillance network by tumour-derived MYC mutants. Nature *436*, 807–811.

Hu, Y., Chen, Y., Douglas, L., and Li, S. (2009). beta-Catenin is essential for survival of leukemic stem cells insensitive to kinase inhibition in mice with BCR-ABL-induced chronic myeloid leukemia. Leukemia *23*, 109–116.

Hu, Y., Liu, Y., Pelletier, S., Buchdunger, E., Warmuth, M., Fabbro, D., Hallek, M., Van Etten, R.A., and Li, S. (2004). Requirement of Src kinases Lyn, Hck and Fgr for BCR-ABL1-induced B-lymphoblastic leukemia but not chronic myeloid leukemia. Nat. Genet. *36*, 453–461.

Hu, Y., Swerdlow, S., Duffy, T.M., Weinmann, R., Lee, F.Y., and Li, S. (2006). Targeting multiple kinase pathways in leukemic progenitors and stem cells is essential for improved treatment of Ph+ leukemia in mice. Proc. Natl. Acad. Sci. U S A *103*, 16870–16875.

Huelsken, J., Vogel, R., Erdmann, B., Cotsarelis, G., and Birchmeier, W. (2001). b-catenin controls hair follicle morphogenesis and stem cell differentiation in the skin. Cell *105*, 533–545.

Hunger, S.P. (2011). Tyrosine kinase inhibitor use in pediatric Philadelphia chromosome-positive acute lymphoblastic anemia. Hematology Am. Soc. Hematol. Educ. Program *2011*, 361–365.

Huntly, B.J., Shigematsu, H., Deguchi, K., Lee, B.H., Mizuno, S., Duclos, N., Rowan, R., Amaral, S., Curley, D., Williams, I.R., et al. (2004). MOZ-TIF2, but not BCR-ABL, confers properties of leukemic stem cells to committed murine hematopoietic progenitors. Cancer Cell *6*, 587–596.

Jamieson, C.H., Ailles, L.E., Dylla, S.J., Muijtjens, M., Jones, C., Zehnder, J.L., Gotlib, J., Li, K., Manz, M.G., Keating, A., et al. (2004). Granulocyte-macrophage progenitors as candidate leukemic stem cells in blast-crisis CML. N. Engl. J. Med. *351*, 657–667.

Jeannet, G., Boudousquie, C., Gardiol, N., Kang, J., Huelsken, J., and Held, W. (2010). Essential role of the Wnt pathway effector Tcf-1 for the establishment of functional CD8 T cell memory. Proc. Natl. Acad. Sci. U S A *107*, 9777–9782.

Jho, E.-H., Zhang, T., Domon, C., Joo, C.-K., Freund, J.-N., and Costantini, F. (2002). Wnt/b-Catenin/Tcf signaling induces the transcription of axin2, a negative regulator of the signaling pathway. Mol. Cell. Biol. *22*, 1172–1183.

Kawauchi, D., Robinson, G., Uziel, T., Gibson, P., Rehg, J., Gao, C., Finkelstein, D., Qu, C., Pounds, S., Ellison, D.W., et al. (2012). A mouse model of the most aggressive subgroup of human medulloblastoma. Cancer Cell *21*, 168–180.

Kim, P.J., Plescia, J., Clevers, H., Fearon, E.R., and Altieri, D.C. (2003). Survivin and molecular pathogenesis of colorectal cancer. Lancet *362*, 205–209.

Kim, Y.M., Ma, H., Oehler, V.G., Gang, E.J., Nguyen, C., Masiello, D., Liu, H., Zhao, Y., Radich, J., and Kahn, M. (2011). The gamma catenin/CBP complex maintains survivin transcription in beta-catenin deficient/depleted cancer cells. Curr. Cancer Drug Targets *11*, 213–225.

Kolly, C., Zakher, A., Strauss, C., Suter, M.M., and Muller, E.J. (2007). Keratinocyte transcriptional regulation of the human c-Myc promoter occurs via a novel Lef/Tcf binding element distinct from neoplastic cells. FEBS Lett. *581*, 1969–1976.

Kovacic, B., Hoelbl, A., Litos, G., Alacakaptan, M., Schuster, C., Fischhuber, K.M., Kerenyi, M.A., Stengl, G., Moriggl, R., Sexl, V., and Beug, H. (2012). Diverging fates of cells of origin in acute and chronic leukaemia. EMBO Mol. Med. *4*, 283–297.

Li, J., Swope, D., Raess, N., Cheng, L., Muller, E.J., and Radice, G.L. (2011). Cardiac tissue-restricted deletion of plakoglobin results in progressive cardiomyopathy and activation of {beta}-catenin signaling. Mol. Cell. Biol. *31*, 1134–1144.

Lu, D., Zhao, Y., Tawatao, R., Cottam, H.B., Sen, M., Leoni, L.M., Kipps, T.J., Corr, M., and Carson, D.A. (2004). Activation of the Wnt signaling pathway in chronic lymphocytic leukemia. Proc. Natl. Acad. Sci. U S A *101*, 3118–3123.

Miravet, S., Piedra, J., Castano, J., Raurell, I., Franci, C., Dunach, M., and Garcia de Herreros, A. (2003). Tyrosine phosphorylation of plakoglobin causes contrary effects on its association with desmosomes and adherens junction components and modulates beta-catenin-mediated transcription. Mol. Cell. Biol. *23*, 7391–7402.

Morgan, R.G., Pearn, L., Liddiard, K., Pumford, S.L., Burnett, A.K., Tonks, A., and Darley, R.L. (2012). gamma-Catenin is overexpressed in acute myeloid leukemia and promotes the stabilization and nuclear localization of beta-catenin. Leukemia *27*, 336–343.

Muller-Tidow, C., Steffen, B., Cauvet, T., Tickenbrock, L., Ji, P., Diederichs, S., Sargin, B., Kohler, G., Stelljes, M., Puccetti, E., et al. (2004). Translocation products in acute myeloid leukemia activate the Wnt signaling pathway in hematopoietic cells. Mol. Cell. Biol. *24*, 2890–2904.

Mullighan, C.G., Miller, C.B., Radtke, I., Phillips, L.A., Dalton, J., Ma, J., White, D., Hughes, T.P., Le Beau, M.M., et al. (2008). BCR-ABL1 lymphoblastic leukaemia is characterized by the deletion of Ikaros. Nature *453*, 110–114.

Niu, C.C., Zhao, C., Yang, Z.D., Zhang, X.L., Wu, W.R., Pan, J., Zhao, C., Li, Z.Q., Ding, W., Yang, Z., and Si, W.K. (2013). Downregulation of gamma-catenin inhibits CML cell growth and potentiates the response of CML cells to imatinib through beta-catenin inhibition. Int. J. Mol. Med. *31*, 453–458.

O'Hare, T., Zabriskie, M.S., Eiring, A.M., and Deininger, M.W. (2012). Pushing the limits of targeted therapy in chronic myeloid leukaemia. Nat. Rev. Cancer *12*, 513–526.

Pomerantz, M.M., Ahmadiyeh, N., Jia, L., Herman, P., Verzi, M.P., Doddapaneni, H., Beckwith, C.A., Chan, J.A., Hills, A., Davis, M., et al. (2009). The 8q24 cancer risk variant rs6983267 shows long-range interaction with MYC in colorectal cancer. Nat. Genet. *41*, 882–884.

Quentmeier, H., Eberth, S., Romani, J., Zaborski, M., and Drexler, H.G. (2011). BCR-ABL1-independent PI3Kinase activation causing imatinib-resistance. J. Hematol. Oncol. *4*, 6.

Reavie, L., Buckley, S.M., Loizou, E., Takeishi, S., Aranda-Orgilles, B., Ndiaye-Lobry, D., Abdel-Wahab, O., Ibrahim, S., Nakayama, K.I., and Aifantis, I.

(2013). Regulation of c-Myc ubiquitination controls chronic myelogenous leukemia initiation and progression. Cancer Cell *23*, 362–375.

Reya, T., O'Riordan, M., Okamura, R., Devaney, E., Willert, K., Nusse, R., and Grosschedl, R. (2000). Wnt signaling regulates B lymphocyte proliferation through a LEF-1 dependent mechanism. Immunity *13*, 15–24.

Rix, U., Hantschel, O., Durnberger, G., Remsing Rix, L.L., Planyavsky, M., Fernbach, N.V., Kaupe, I., Bennett, K.L., Valent, P., Colinge, J., et al. (2007). Chemical proteomic profiles of the BCR-ABL inhibitors imatinib, nilotinib, and dasatinib reveal novel kinase and nonkinase targets. Blood *110*, 4055–4063.

Roumiantsev, S., de Aos, I.E., Varticovski, L., Ilaria, R.L., and Van Etten, R.A. (2001). The src homology 2 domain of Bcr/Abl is required for efficient induction of chronic myeloid leukemia-like disease in mice but not for lymphoid leukemogenesis or activation of phosphatidylinositol 3-kinase. Blood *97*, 4–13.

Ruiz, P., Brinkmann, V., Ledermann, B., Behrend, M., Grund, C., Thalhammer, C., Vogel, F., Birchmeier, C., Günthert, U., Franke, W.W., and Birchmeier, W. (1996). Targeted mutation of plakoglobin in mice reveals essential functions of desmosomes in the embryonic heart. J. Cell. Biol. *135*, 215–225.

Schmitz, M., Breithaupt, P., Scheidegger, N., Cario, G., Bonapace, L., Meissner, B., Mirkowska, P., Tchinda, J., Niggli, F.K., Stanulla, M., et al. (2011). Xenografts of highly resistant leukemia recapitulate the clonal composition of the leukemogenic compartment. Blood *118*, 1854–1864.

Schurch, C., Riether, C., Matter, M.S., Tzankov, A., and Ochsenbein, A.F. (2012). CD27 signaling on chronic myelogenous leukemia stem cells activates Wnt target genes and promotes disease progression. J. Clin. Invest. *122*, 624–638.

Signer, R.A., Montecino-Rodriguez, E., Witte, O.N., and Dorshkind, K. (2010). Immature B-cell progenitors survive oncogenic stress and efficiently initiate Ph+ B-acute lymphoblastic leukemia. Blood *116*, 2522–2530.

Trumpp, A., Refaeli, Y., Oskarsson, T., Gasser, S., Murphy, M., Martin, G.R., and Bishop, J.M. (2001). c-Myc regulates mammalian body size by controlling cell number but not cell size. Nature *414*, 768–773.

Tuupanen, S., Turunen, M., Lehtonen, R., Hallikas, O., Vanharanta, S., Kivioja, T., Bjorklund, M., Wei, G., Yan, J., Niittymaki, I., et al. (2009). The common colorectal cancer predisposition SNP rs6983267 at chromosome 8q24 confers potential to enhanced Wnt signaling. Nat. Genet. *41*, 885–890.

Tyner, J.W., Jemal, A.M., Thayer, M., Druker, B.J., and Chang, B.H. (2012). Targeting survivin and p53 in pediatric acute lymphoblastic leukemia. Leukemia *26*, 623–632.

van Genderen, C., Okamura, R.M., Farinas, I., Quo, R.-G., Parslow, T.G., Bruhn, L., and Grosschedl, R. (1994). Development of several organs that require inductive epithelia-mesenchymal interactions is impaired in LEF-1 deficient mice. Genes Dev. *8*, 2691–2703.

Verbeek, S., Izon, D., Hofhuis, F., Robanus-Maandag, E., te Riele, H., van de Wetering, M., Oosterwegel, M., Wilson, A., MacDonald, H.R., and Clevers, H. (1995). An HMG-box-containing T-cell factor required for thymocyte differentiation. Nature *374*, 70–74.

Wang, Y., Krivtsov, A.V., Sinha, A.U., North, T.E., Goessling, W., Feng, Z., Zon, L.I., and Armstrong, S.A. (2010). The Wnt/beta-catenin pathway is required for the development of leukemia stem cells in AML. Science *327*, 1650–1653.

Williamson, L., Raess, N.A., Caldelari, R., Zakher, A., de Bruin, A., Posthaus, H., Bolli, R., Hunziker, T., Suter, M.M., and Muller, E.J. (2006). Pemphigus vulgaris identifies plakoglobin as key suppressor of c-Myc in the skin. EMBO J. *25*, 3298–3309.

Yeung, J., Esposito, M.T., Gandillet, A., Zeisig, B.B., Griessinger, E., Bonnet, D., and So, C.W. (2010). beta-Catenin mediates the establishment and drug resistance of MLL leukemic stem cells. Cancer Cell *18*, 606–618.

Yochum, G.S., Cleland, R., and Goodman, R.H. (2008). A genome-wide screen for beta-catenin binding sites identifies a downstream enhancer element that controls c-Myc gene expression. Mol. Cell. Biol. *28*, 7368–7379.

Zhao, C., Blum, J., Chen, A., Kwon, H.Y., Jung, S.H., Cook, J.M., Lagoo, A., and Reya, T. (2007). Loss of beta-catenin impairs the renewal of normal and CML stem cells in vivo. Cancer Cell *12*, 528–541.

Zheng, X., Beissert, T., Kukoc-Zivojnov, N., Puccetti, E., Altschmied, J., Strolz, C., Boehrer, S., Gul, H., Schneider, O., Ottmann, O.G., et al. (2004). Gamma-catenin contributes to leukemogenesis induced by AML-associated translocation products by increasing the self-renewal of very primitive progenitor cells. Blood *103*, 3535–3543.

STAR★METHODS

KEY RESOURCES TABLE

REAGENT or RESOURCE	SOURCE	IDENTIFIER
Antibodies		
Anti-Mouse CD3e	eBioscience	Cat#56-0032-82; RRID: AB_467055
Anti-Mouse CD3e	eBioscience	Clone 145-2C11; RRID: AB_11149861
Anti-Mouse CD4	eBioscience	Clone GK1.5; RRID: AB_493999
Anti-Mouse CD8a	eBioscience	Clone 53-6.7; RRID: AB_2534400
Anti-mouse CD11b	Biolegend	Clone M1/70; RRID: AB_312790
Anti-mouse CD16/32	in house	Clone 2.4G2
Anti-Mouse CD19	eBioscience	Clone eBio1D3; Cat#56-0193-82
Anti-mouse CD34	eBioscience	Clone Ram34; RRID: AB_657739
Anti-mouse CD43 PE	BD Biosciences	Cat#553271; RRID: AB_394748
Anti-mouse CD45	in house	Clone M1/89
Anti-mouse CD45 eFluor450	eBioscience	Clone 30-F11; RRID: AB_10597009
Anti-mouse CD45R (B220)	eBioscience	Clone RA3-6B2
Anti-Mouse CD45.1	eBioscience	Clone A20; RRID: AB_1272189
Anti-Mouse CD45.2	eBioscience	Clone 104.2; RRID: AB_953590
Anti-mouse CD117 PeCy7 (c-kit)	eBioscience	Clone 2B8 RRID: AB_469645
Anti-Mouse CD127	eBioscience	Clone A7R34 RRID: AB_469435
Anti-mouse CD249 (BP-1)	BD Biosciences	Cat#564533; RRID: AB_2738838
Anti-mouse IgM	BD Biosciences	Cat#553436; RRID: AB_394856
Anti-mouse IgM	BD Biosciences	Cat#553409; RRID: AB_394845
Anti-mouse GR1	eBiosciences	Cat#56-5931-82; RRID: AB_494007
Anti-mouse Sca1 APC	in house	Clone D7
Anti-mouse Ter119	BD Biosciences or in house	Cat#560509; RRID: AB_164230
Rabbit anti-mouse/human MYC	Abcam	Cat#ab32072; RRID: AB_731658
Rabbit anti-mouse BIRC5 (Survivin)	Cell Signaling	Cat#2808; RRID: AB_2063948
Rabbit anti-human BIRC5 (Survivn)	Abcam	Cat#Ab76424; RRID: AB_1524459
Rabbit anti-human p21 (CDKN1A)	Cell Signaling	Cat#2947; RRID: AB_823586

(*Continued on next page*)

Continued

REAGENT or RESOURCE	SOURCE	IDENTIFIER
Anti-human CD19 PE	BioLegend	Clone HIB19; RRID: AB_314237
Anti-human CD45 Alexa Flour 647	BioLegend	Clone HI30; RRID: AB_493034
Anti-human b2 microglobulin PE (Clone Tü99)	BD Biosciences	Cat#551337; RRID: AB_394152
Fab2 donkey anti-rabbit IgG PE	eBioscience	Cat#12-4739-81; RRID: AB_1210761
Anti-mouse/human γ–catenin (Western Blot)	BD Biosciences	Clone 15; RRID: AB_397649
Anti-mouse/human b-catenin (Western Blot)	BD Biosciences	Clone 14; RRID: AB_397554
Anti-human ABL (Western Blot)	Abcam	Cat# ab16905; RRID: AB_443541
Anti-mouse/human beta-actin (Western Blot)	Sigma	Cat#A1978; RRID: AB_476692
Anti-influenza hemagglutinin (HA) (Western Blot)	Roche	Clone 3F10; RRID: AB_10094468
anti-human MYC (Western Blot)	Sigma	Clone 9E10; RRID: AB_439694
anti-phospho Tyrosine (pTyr) (Western Blot)	Millipore	Clone 4G10; RRID: AB_309678
goat anti-rabbit IgG HRP (Western Blot)	Southern Biotech	Cat#4030-05; RRID: AB_2687483
goat anti-rat IgG HRP (Western Blot)	Southern Biotech	Cat# 3030-05; RRID: AB_2716837
goat anti-mouse IgG1 HRP (Western Blot)	Southern Biotech	Cat#1071-05; RRID: AB_2794426
goat anti-mouse IgG2a HRP (Western Blot)	Southern Biotech	Cat#1081-05; RRID: AB_2736843
mouse anti-human γ-catenin (ChIP)	BD Biosciences	Cat#610253; RRID: AB_397648
rabbit anti-human b-catenin (polyclonal) (ChIP)	Santa Cruz Biotechnology	Cat#sc-7199; RRID: AB_634603
anti-human LEF1 (polyclonal) (ChIP)	Santa Cruz Biotechnology	Cat#sc-8591; RRID: AB_21356
rabbit IgG (ChIP)	Millipore	Cat#12-370; RRID: AB_145841
Chemicals, Peptides, and Recombinant Proteins		
AnnexinV- PE	eBioscience	Cat#88-8102-72
Aqua dead	Invitrogen	Cat#L34966
Biotin	Sigma	Cat#B4501
DAPI	Molecular Probes	Cat#D1306
ECL	GE Healthcare	Cat#RPN2106
Femto ECL	Thermo Scientific	Cat#34095
Hoechst	Molecular Probes	Cat#H3570
human IL-7	Peprotech	Cat#200-07
Inhibitor: Imatinib	Symansis	Cat#SY-Imatinibmesylate
Inhibitor: Dasatinib	Symansis	Cat#SY-Dasatinib
Inhibitor: Nilotinib	Symansis	Cat#SY-Nilotinib
Inhibitor: SU6656	EMDMillipore	Cat#572635
Magnetic beads	Lifetechnologies	Cat #10001D
murine IL-7	Peprotech	Cat#217-17

(*Continued on next page*)

Continued

REAGENT or RESOURCE	SOURCE	IDENTIFIER
murine Stem cell factor (SCF)	Peprotech	Cat#250-03
murine TPO (Thrombopoietin)	Peprotech	Cat# 315-14
Polybrene (Hexadimthrine bromide)	Sigma Aldrich	Cat#H9268
Puromycin	Sigma Aldrich	Cat#P8833
Polyinosinic-polycytodylic acid (polyI:C)	Invivogen	Cat#vac-pic
Protein A+G magnetic beads	Millipore	Cat#16-663
Strep-Tactin Sepharose beads	IBA Lifesciences	Cat#2-1201-010
Sytox blue	Thermo Scientific	Cat#S34857
7-AAD	Biolegend	Cat#420403
Critical Commercial Assays		
BrdU flow kit	BD	Cat#51-2354AK
FoxP3/Transcription factor staining buffer	Invitrogen	Cat#00-5523-00
LightCycler FastStart DNA Master SYBR Green I	Roche	Cat#12239264001
MethoCult	StemCell Technologies	Cat#M3234
Mouse hematopoietic progenitor cell isolation kit	StemCell Technologies	Cat#19856
Superscript III first strand kit	Invitrogen	Cat#18080-501
Deposited Data		
Gene array data of *Jup*$^{+/+}$ versus *Jup*$^{-/-}$ BCR-ABL1^{+} preleukemic B cells	This study	GEO: GSE54793
Experimental Models: Cell Lines		
Human: NALM-1	DSMZ, Germany	ACC-131
Human: SD-1	A. Ochsenbein (UniBE)	
Human: Sup-B15	DSMZ, Germany	ACC-389
Human: BV-173	DSMZ, Germany	ACC-20
Human: TOM-1	DSMZ, Germany	ACC 578
Human: K562	DSMZ, Germany	ACC-10
Human: REH	DSMZ, Germany	ACC-22
Human: Sem	DSMZ, Germany	ACC-546
Human: 697	DSMZ, Germany	ACC-42
Experimental Models: Organisms/Strains		
Mouse: *Jup*$^{+/-}$	(Ruiz et al., 1996)	
Mouse: *Jup*^{lox}	(Li et al., 2011), G. Radice, Philadelphia and E. Mueller, Bern)	
Mouse: *Ctnnb1*^{lox}	(Huelsken et al., 2001), W. Birchmeier, Berlin	
Mouse: *Myc*^{lox}	(Trumpp et al., 2001), A. Trumpp, Heidelberg	
Mouse: B6.129-Tm(Lef1)Rug	(van Genderen et al., 1994) (R. Grosschedl, Freiburg	
Mouse: B6.129-Tm(Tcf7)Cle (*Tcf7*$^{-/-}$) (CD45.2)	(Verbeek et al., 1995), H. Clevers, Utrecht	RRID: MGI:4360712
Mouse: B6.Cg-Commd10<Tg(Vav1-icre)A2Kio>/J	JAX	Strain 008610
Mouse: B6.Cg-Tg(Mx1-cre)1Cgn/J	JAX	Strain 003556
Mouse: B6.SJL-Ptprc<a> (B6 CD45.1)	JAX	Strain 002014 RRID: MGI:6200621
Mouse: NOD.Cg-Prkdc<scid> Il2rg<tm1Wjl>/SzJ (NSG)	JAX	Strain 005557
Oligonucleotides		
m. Vav-Cre DNA PCR Forward primer: AGATGCCAGGACATCAGGAACCTG	this paper	
m. Vav-Cre DNA PCR Reverse primer: ATCAGCCACACCAGACAC AGAGATC	this paper	

(*Continued on next page*)

Continued

REAGENT or RESOURCE	SOURCE	IDENTIFIER
m. Ctnnb1^{lox} DNA PCR Forward primer:ACTGCCTTTGTTCTCTT CCCTTCTG	this paper	
m. Ctnnb1^{lox} DNA PCR Reverse primer: GAATCCAAGTAAGACTGCTGCTGC	this paper	
m. Ctnnb1$^{\Delta}$ DNA PCR Forward primer:ACTGCCTTTGTTCTCTTC CCTTCTG	this paper	
m. Ctnnb1$^{\Delta}$ DNA PCR Reverse primer: CTTGTTGCTAGAGCAGACAGACAG	this paper	
m. Jup DNA PCR Forward primer:CTTCTATCGCCTTCTTGACG	this paper	
m. Jup DNA PCR Reverse primer:CGGCCATCGTCCATCTCATC	this paper	
m. Jup DNA PCR Reverse primer:CCTCCTTCTTGGACAGCTGG	this paper	
m. Lef1 DNA PCR Forward primer:CCGTTTCAGTGGCACGCCCTCTCC	this paper	
m. Lef1 DNA PCR Forward primer:ATGGCGATGCCTGCTTGCCGAATA	this paper	
m. Lef1 DNA PCR Reverse primer:TGTCTCTCTTTCCGTGCTAGTTC	this paper	
m. Tcf7 DNA PCR Forward primer:ATGGCGATGCCTGCTTGCCGA ATATGC	this paper	
m. Tcf7 DNA PCR Reverse primer: TGAGTGCACACTCAAGG	this paper	
m. Tcf7 DNA PCR Reverse primer: GTAGTTATCCCGCGCGGA CC	this paper	
m. Myc^{lox} DNA PCR Forward primer:GCATTTTAATTCCAGCGCATCAG	this paper	
m. Myc^{lox} DNA PCR Reverse primer: ACAACGTCTTGGAACGTCAGAGG	this paper	
m. Myc$^{\Delta}$ DNA PCR Forward primer:TTTCTGACTCGCTGTAGTAATTCC	this paper	
m. Myc$^{\Delta}$ DNA PCR Reverse primer:AGGCAGTTAAAATTATGGCTGAAG	this paper	
m. Myc$^{\Delta}$ DNA PCR Reverse primer: CACCGCCTACATCCTGTCCATTC	this paper	
m. Jup^{lox} DNA PCR Forward primer:AAGAAATACCCACGGCTCCT	this paper	
m. Jup^{lox} DNA PCR Reverse primer: GCTCCAGGGAGAAACAGA CA	this paper	
m. Jup$^{\Delta}$ DNA PCR Forward primer:AAG AAA TAC CCA CGGCTCCT	this paper	
m. Jup$^{\Delta}$ DNA PCR Reverse primer: TTCGACGGAGTAGCATAGGG	this paper	
m. Mx-Cre DNA PCR Forward primer:AAAGCAGGCAGCCATCTGAAC	this paper	
m. Mx-Cre DNA PCR Reverse primer: TCTTGCGAACCTCATCACTCG	this paper	
m. Tcf7 qPCR Forward primer:AGCTTTCTCCACTCTACGAACA	this paper	
m. Tcf7 qPCR Reverse primer: AATCCAGAGAGATCGGGGGTC	this paper	
m. Lef1 qPCR Forward primer:CTGGTCAGCGCGAGACAATTA	this paper	
m. Lef1 qPCR Reverse primer: CTTTGCACGTTGGGAAGGA	this paper	
m. Tcf7L1 qPCR Forward primer:ACGAGCTGATCCCCTTCCA	this paper	
m. Tcf7L1 qPCR Reverse primer: CAGGGACGACTTGACCTCAT	this paper	
m. Tcf7L2 qPCR Forward primer:CGAAAAGTTCCTCCGGGTTTG	this paper	
m. Tcf7L2 qPCR Reverse primer: CGTAGCCGGGCTGATTCAT	this paper	
m. Jup qPCR Forward primer:GACTACCACCTATACACAAGGGG	this paper	
m. Jup qPCR Reverse primer: AGCAGTAGAGAACTGTCCTCG	this paper	
m. Lgr5 qPCR Forward primer:CCAATGGAATAAAGACGACGGCAACA	this paper	
m. Lgr5 qPCR Reverse primer: GGGCCTTCAGGTCTTCCTCAAAGTCA	this paper	
m. Axin2 qPCR Forward primer:TGACTCTCCTTCCAGATCCCA	this paper	
m. Axin2 qPCR Reverse primer: TGCCCACACTAGGCTGACA	this paper	
m. Myc qPCR Forward primer: GGACAGTGTTCTCTGCC	this paper	

(*Continued on next page*)

Continued

REAGENT or RESOURCE	SOURCE	IDENTIFIER
m. Myc qPCR Reverse primer: CGTCGCAGATGAAATAGG	this paper	
h. BIRC5 qPCR Forward primer:GCCTGGCAGCCCTTTCTC	this paper	
h. BIRC5 qPCR Reverse primer: GCCAGCTGCTCGATGGC	this paper	
m. TBP qPCR Forward primer:CCTTCACCAATG ACTCCTATGAC	this paper	
m. TBP qPCR Reverse primer: CAAGTTTACAGCCAAGATTCAC	this paper	
m. HPRT qPCR Forward primer:GTTGGATACAGGCCAGACTTTGTTG	this paper	
m. HPRT qPCR Reverse primer: GATTCAACTTGCGCTCATCTTAGGC	this paper	
h. MYC TBE1 CHIP-qPCR Forward primer: TCACAAGGGTCTCTG CTGACTC	this paper	
h. MYC TBE1 CHIP-qPCR Reverse primer: GGGTTTGGGAGAAAT CAAAGGT	this paper	
h. MYC TBE2 CHIP-qPCR Forward primer: GCGCCCATTAATA CCCTTCTTT	this paper	
h. MYC TBE2 CHIP-qPCR Reverse primer: TCCACACCGAGA ACGCACT	this paper	
h. MYC TBE3&4 CHIP-qPCR Forward primer: GGGAGATCCG GAGCGAATA	this paper	
h. MYC TBE3&4 CHIP-qPCR Reverse primer: TCGGGTGTTGT AAGTTCCAGTG	this paper	
h. MYC TBE5 CHIP-qPCR Forward primer: GGCGCTCTTAAA CAGCTCAGTC	this paper	
h. MYC TBE5 CHIP-qPCR Reverse primer: CAGACTAACACC TTCCCGATTCC	this paper	
h. MYC 5' enhancer CHIP-qPCR Forward primer: GAGGGACGA ATAAACTCTCCTCCT	this paper	
h. MYC 5' enhancer CHIP-qPCR Reverse primer: TCAGTGCC TTTCATCTGCTGAG	this paper	
h. MYC 5' upstream control CHIP-qPCR Forward primer: CCTT CACCTCATCTCTTGACAGG	this paper	
h. MYC 5' upstream control CHIP-qPCR Reverse primer: AAAG CAACTGGACGTGGTGAA	this paper	
h. AXIN2 TBE2 CHIP-qPCR Forward primer: GCTTTGATAAGG TCCTGGCAAC	this paper	
h. AXIN2 TBE2 CHIP-qPCR Reverse primer: CCGAAATCCATC GCTCTGA	this paper	
h. AXIN2 TBE3 CHIP-qPCR Forward primer: CGCCTTTGAAGT GCACAGTTA	this paper	
h. AXIN2 TBE3 CHIP-qPCR Reverse primer: AGGTCCTGTTTC CAGCAGTCAC	this paper	
h. AXIN2 5' upstream control CHIP-qPCR Forward primer: AGGCTAGAGAGAGGGCTTTCCA	this paper	
h. AXIN2 5' upstream control CHIP-qPCR Reverse primer: AACAGGTGCTCGGGTCACTTTA	this paper	
Recombinant DNA		
Plasmid: MSCV-BCR-ABL1 (p210)-IRES-GFP	X. Jiang, Terry Fox Laboratory	
Plasmid: MSCV-BCR-ABL1 (p210)-IRES-mCherry	this paper	
Plasmid: MSCV-BCR-ABL1 (p185)-IRES-GFP	O. Hantschl, EPFL	
Plasmid: MSCV-IRES-GFP	J. Huelsken, EPFL	
Plasmid: MSCV-MYC-IRES-GFP	(Hemann et al., 2005), S. Lowe	RRID: Addgene_18770
Plasmid: MSCV-pBabeMCS-IRES-RFP	M. Roussel and C. Sherr	RRID: Addgene_33337
Plasmid: MSCV-MYC-IRES-RFP	(Kawauchi et al., 2012), M. Roussel	RRID: Addgene_35395
Plasmid: pLKO Sh JUP (human) (Sh JUP1)	Open Biosystems	TRCN0000083709

(*Continued on next page*)

Continued

REAGENT or RESOURCE	SOURCE	IDENTIFIER
Plasmid: pLKO Sh JUP (human) (Sh JUP2)	Open Biosystems	TRCN0000083710
Plasmid: pLKO Sh b-catenin (human)	Open Biosystems	TRCN0000003843
Plasmid: pLKO Sh b-catenin (human)	Open Biosystems	TRCN0000003845
Plasmid: pLKO Sh MYC (human)	Open Biosystems	TRCN0000174055
Plasmid: pLKO Sh MYC (human)	Open Biosystems	TRCN0000010390
Plasmid: pLKO Sh scrambled (Sh scr)	Sigma	SHC002
Plasmid: pCL Eco (Retrovirus production)	Imgenex	Cat# 10045P
Plasmid: pCL Ampho (Retrovirus production)	B. Reina, Strasbourg	
Plasmid: pCMVR8.74 (Lentivirus production)	D. Trono, EPFL	RRID: Addgene_22036
Plasmid: pMD2.G (Lentivirus production)	D. Trono, EPFL	RRID: Addgene_12259
Plasmid: Lenti pgk-BIRC5-T2A-GFP	this paper	
Plasmid: MSCV BIRC5 IRES-RFP	this paper	
Plasmid: Lenti MYC-γ-catenin (human)	this paper	
Plasmid: Lenti MYC-γ-catenin resistant to Sh JUP1 (TRCN0000083709)	this paper	
Plasmid: Lenti MYC-γ-catenin resistant to Sh JUP2 (TRCN0000083710)	this paper	
Plasmid: Lenti MYC-γ-catenin mut (Y133/550/644F)	this paper	
Plasmid: Lenti MYC-γ-catenin mut (Y133/550/644F) resistant to Sh JUP1 (TRCN0000083709)	this paper	
Plasmid: Lenti mPgk SBP-HA-g-catenin hPgk GFP	this paper	
Plasmid: Lenti mPgk SBP-HA-g-catenin mut hPgk GFP	this paper	
Plasmid: Lenti hU6 Sh JUP1 hPgk RFP	this study	
Plasmid: Lenti hU6 Sh JUP1 hPgk Cerulean	this study	
Plasmid: Lenti hU6 Sh JUP2 hPgk RFP	this study	
Plasmid: Lenti hU6 Sh JUP2 hPgk Cerulean	this study	
Plasmid: Lenti hU6 Sh scr hPgk RFP	this study	
Plasmid: Lenti hU6 Sh scr hPgk Cerulean	this study	
Software and Algorithms		
GraphPad Prism	http://graphpad-prism.software.informer.com/5.0/,	RRID: SCR_002798
FlowJo	Tree Star	RRID: SCR_008520
Fiji	https://github.com/fiji/fiji	RRID: SCR_002285
Adobe Photoshop	Adobe	http://www.adobe.com/legal/terms.html
LightCycler data analysis software, Version 3.5	Roche	
GeneGO MetaCore analysis software	http://www.genego.com/metacore.php	RRID: SCR_008125
ImageJ		RRID: SCR_003070

CONTACT FOR REAGENT AND RESOURCE SHARING

Further information and requests for resources and reagents should be directed to and will be fulfilled by the Lead Contact, Werner Held (Werner.Held@unil.ch).

EXPERIMENTAL MODEL AND SUBJECT DETAILS

Animal experiments were conducted in accordance with protocols approved by the veterinary authorities of the Canton de Vaud and the Kanton Zurich, Switzerland. Mouse strains were maintained in the SPF animal facilities of the University of Lausanne or the University of Zurich. Donor and irradiated recipients of bone marrow cells were sex matched. Recipients were >6 weeks of age.

Animal experiments were conducted in accordance with protocols approved by the veterinary authorities of the Canton de Vaud and the Canton of Zurich, Switzerland.

The studies involving human subjects were approved by the ethics commission of the Kanton Zurich (approval number 2014-0383) and informed consent was obtained from all subjects in accordance with the Declaration of Helsinki. Primary human ALL cells were from cryopreserved bone marrow aspirates from patients enrolled in the ALL-BFM 2000 study.

METHOD DETAILS

Mouse Strains

Jup$^{+/-}$ (Ruiz et al., 1996), *Jup*$^{lox/lox}$ (Li et al., 2011), *Ctnnb1*$^{lox/lox}$ (Huelsken et al., 2001), *Myc*^{lox} (Trumpp et al., 2001), *Lef1*$^{+/-}$ (van Genderen et al., 1994), *Tcf7*$^{-/-}$ (Verbeek et al., 1995) have been described. *Vav-Cre*, *Mx1-Cre* transgenic, CD45.1 congenic C57BL/6 (B6) and NOD *Prkdc*^{scid} *Il2rg*$^{-/-}$ (NSG) mice were obtained from the Jackson Lab (Bar Harbor, ME)

Fetal Liver Chimeras

Fetal liver cells from intercrosses of *Jup*$^{+/-}$ or *Lef1*$^{+/-}$ mice (CD45.2) were obtained at day 13.5 and of day 14-16 of gestation, respectively. Following genotyping by PCR appropriate fetal liver cells were injected into irradiated (900rad) B6 recipients (CD45.1). Recipients were allowed to engraft for 6 to 8 weeks before further use. Hematopoietic cells in recipient mice were largely donor-derived (>95% CD45.2^{+}) use.

Constructs, Viral Vectors, Virus Production and Stable Transfectants

Constructs: MSCV-BCR-ABL1 (p210)-IRES-GFP (X. Jiang, Terry Fox Laboratory), MSCV-BCR-ABL1 (p210)-IRES-mCherry, MSCV-BCR-ABL1 (p185)-IRES-GFP (O. Hantschl, EPFL), MSCV-IRES-GFP, MSCV-MYC-IRES-GFP (a gift from Scott Lowe (Addgene plasmid # 18770), pMSCV-pBabeMCS-IRES-RFP (gift from Martine Roussel & Charles Sherr (Addgene plasmid # 33337)), MSCV-MYC-IRES-RFP (a gift from Martine Roussel (Addgene plasmid # 35395), Lentivirus-pgk-BIRC5-T2A-GFP (codon optimized *BIRC5* synthesized by Cyagen, this paper), MSCV-BIRC5 IRES-RFP vector (this paper). Lenti based knockdown constructs (listed in the Key Resources Table) were purchased form Open Biosystems or Sigma.

Point mutations that change tyrosines (Y) at position 133, 550 and 644 to phenylalanine (F) and/or three point mutations that render γ-catenin resistant to Sh JUP1 (available upon request) were introduced into a MYC-tagged γ-catenin cDNA. Point mutations that render γ-catenin resistant to Sh JUP 2 (available upon request) were introduced into a MYC-tagged γ-catenin cDNA. A streptavidin-Binding Peptide (SBP) and three copies of the HA tag were added to the N-terminus of γ-catenin. All constructs were introduced into lentivirus vector with a bidirectional a muPgk promoter driving GFP and γ-catenin.

Virus production: For the production of retroviruses, 293T cells were transiently transfected with mouse stem cell virus (MSCV) vectors plus pCL Eco or pCL Ampho packaging plasmids. For the production of lentiviruses, 293T cells were transiently transfected with second or third generation packaging plasmids. After concentration of culture supernatants using filter columns (Millipore), virus supernatants were either used directly or stored frozen. Infected cells were flow sorted based on GFP or RFP fluorescence to obtain stably transduced Ph^{+} cell variants.

Murine Ph^{+} Leukemia

Ph^{+} B-ALL was induced according to (Roumiantsev et al., 2001). Total BM cells (CD45.2^{+}) were cultured in RPMI (Invitrogen), 10% FCS, 10mM HEPES, 10 ng/ml IL-7 (R&D Systems), 10% WEHI-3B supernatant (containing IL-3), 5 μg/ml polybrene and concentrated supernatant containing MSCV BCR-ABL1 (p210) or (p185) IRES GFP or mCherry. After 1 hr the cells were washed and 10^6 cells were injected i.v. into irradiated C57BL/6 (B6) (CD45.1) recipients. To analyze B-ALL initiation from B lineage committed cells, B220^{+} CD19^{+} IgM^{-} cells were flow sorted after the 1 hr infection and $5x10^5$ B cells (CD45.2) were injected into irradiated WT recipient mice (CD45.1) together with WT rescue BM cells ($2.5x10^5$) (CD45.1).

Deletion of *Jup* was induced by 3 injections of polyinosinic-polycytodylic acid (poly(I:C) (pIC)) (250μg/dose) (Invivogen) on day 7, 9, and 11 post transplantation of transduced BM.

CML-like disease using enriched HSC was induced according to (Reavie et al., 2013). Lineage marker negative (Lin^{-}) cells were purified from BM using the mouse hematopoietic progenitor cell isolation kit (Stemcell Technology). Lin^{-} Sca-1^{+} c-Kit^{+} (LSK) cells were flow sorted, pre-stimulated overnight in Opti-MEM 10% FCS, 10mM HEPES, mSCF (100 ng/ml) and TPO (20 ng/ml) (Peprotech) and infected with MSCV BCR-ABL1 (p210) IRES GFP for 4 hr. The infection was repeated the next day and one day later $4x10^4$ cells (CD45.2) were injected into irradiated WT recipient mice (CD45.1) together with WT rescue BM ($2.5x10^5$) (CD45.1).

Flow Cytometry

BM and spleen cell suspensions were treated with ACK buffer to remove erythrocytes and incubated with 2.4G2 (anti-CD16/32) hybridoma supernatant to block Fc receptors. mAbs used for multi-color flow cytometry are listed in the Key Resources Table. Abs were conjugated to appropriate fluorochromes (FITC, PE, PE-Texas red, PE-Cy5, PE-Cy5.5, PerCP-Cy5.5, PE-Cy7, APC, Alexa647, Alexa700, APC-Cy7, APC-Alexa780, Pacific blue, efluor450 or Pacific orange) in house or were purchased from

eBiosciences, Becton Dickinson (BD) or Biolegend. 7AAD (eBiosciences), DAPI (Molecular Probes), Sytox blue (Molecular Probes) or Aqua dead (Invitrogen) were used to gate out dead cells. Cocktail of PE-Cy7- or AF700-conjugated anti-CD3e (17A2), CD4 (GK1.5), CD8a (53.6.7), CD11b (MI/70), CD19 (eBio1D3), B220 (RA3-6B2), GR-1 (RB6-8C5), Ter119 (Ter11)) mAbs were used to gate out lineage-positive cells.

For cell proliferation assays, mice were injected with 100μl BrdU (BrdU flow kit, BD), and sacrificed 1 hr later. The staining was performed according to manufacturer's instructions. For the analysis of cell death, BM cells and splenocytes were incubated for 2 hr at 37°C in RPMI plus 10% FCS in the absence of growth factors, before cell surface and AnnexinV-Cy-5 (BD) staining. Sytox blue (Molecular Probes) was added to identify dead cells.

For MYC and BIRC5 (Survivin) detection, human Ph^+ cells were fixed with 80% and 100% methanol, respectively, and resuspended in PBS 0.1% Tween. Goat serum was used to prevent non-specific binding before incubation with rabbit anti-MYC (Ab32072, Abcam) or rabbit anti-human BIRC5 (Ab76424, Abcam). For p21 staining cells were fixed using the Foxp3/Transcription Factor Staining Buffer kit (eBioscience) and incubated with rabbit anti-human p21 (2947S, Cell signaling). For BIRC5 detection in murine Ph^+ tumor samples, frozen splenocytes were thawed and Live dead dye^- $CD45.2^+$ $CD45.1^-$ $B220^+$ cells were flow sorted. Sorted cells were fixed with 100% methanol or using the Foxp3/Transcription Factor Staining Buffer kit (ebioscience) and then stained using rabbit anti-mouse BIRC5 (Survivin) (2808T, Cell signaling). For MYC detection in murine LSK cells, BM cells were enriched in hematopoietic progenitors using the mouse hematopoietic progenitor cell isolation kit (StemCell technology, 19856) following provider's protocol. LSK cells were flow sorted, fixed with 80% methanol, resuspended in PBS 0.1%Tween, blocked using goat serum and stained using rabbit anti-MYC (Ab32072, Abcam). Bound primary rabbit antibodies were detected using PE-conjugated anti-rabbit antibody (12-4739, eBioscience) and DAPI was added to exclude sub G_0/G_1 cells.

Samples were run on FACScanto or LSRII flow cytometers (BD), and data were analyzed using the FlowJo software package. For cell sorting the indicated cell types were stained as described above and sorted using a FACSAria (BD) cell sorter. The purity was generally >99% upon reanalysis.

PCR

Analysis of genomic DNA analysis was performed using Hot Start Kapa Mouse genotyping Kit (Kapa Biosystem) using the primers listed in the Key Resources Table.

For RTqPCR, total cellular RNA was purified using TRizol reagent (Invitrogen) and reverse-transcribed using random hexamers and Superscript III first strand kit (Invitrogen). Real-time PCR was performed using the LightCycler FastStart DNA Master SYBR Green I (Roche) according to the instruction manual. Primers are listed in the Key Resources Table. Transcript levels were normalized to that of TATA-binding protein (TBP) or Hypoxanthine-guanine phosphoribosyltransferase (HPRT). Amplification plots were analyzed using the comparative C_T method with LightCycler data analysis software, Version 3.5 (Roche).

Affymetrix Microarray

Total RNA was isolated from four sets flow sorted *Jup*-sufficient and *Jup*-deficient pre-leukemic B cells ($CD45.2^+$ $CD45.1^-$ GFP^+ (BCR-$ABL1^+$) $B220^+$ $BP\text{-}1^+$) (3 weeks post transplantation) using Trizol (Gibco) and RNeasy (Qiagen) purification following manufacturer's instructions. cDNA was synthesized, amplified and samples were hybridized to Affymetrix GeneChip Mouse Gene 1.0 ST array.

RNA quality was checked with a Bioanalyzer (Agilent) and cDNA was synthetized. Results were analyzed using a linear model, paired analysis. The data were preprocessed with RMA (Robust Multichip Average) normalization. Moderated t-test was used for comparison of the 2 groups with a p value adjustment according to Benjamini-Hochberg method. Technical replicates were averaged for fold-change study. Probe sets with adjusted p value (=FDR, False Discovery Rate) <0.05 were exported to Microsoft Excel and analyzed further using GeneGO MetaCore analysis software. The accession number for the array data reported in this paper is GEO: GSE54793.

Colony Formation

Total BM cells were infected with BCR-ABL1 (p185) before plating in methylcellulose medium (MethoCult M3234, StemCell Technologies) in the absence of growth factor addition ($2.5x10^4$/dish). After 8 days colonies were counted, cells were harvested and replated (10^4 /dish) to assess secondary colony formation and eventually tertiary colony formation.

Cell Culture and Inhibitor Treatment

For characteristics of the cell lines used please see below. K562, BV-173, TOM-1, NALM-1 (DSMZ, Germany) and SD-1 (A. Ochsenbein, University of Bern) were cultured in RPMI supplemented with 10% FCS, 1% PS and 10mM HEPES. Sup-B15 (DSMZ, Germany) cells were grown in IMDM (Invitrogen) supplemented with 15% FCS, 1% PS and 10mM HEPES.

To inhibit tyrosine phosphorylation: Sup-B15 cells expressing HA-SBP-tagged γ-catenin were treated for 6 hr with Imatinib (inhibits ABL kinases and a few receptor tyrosine kinases, 10μM), Nilotinib (selectively more potent for ABL, 1μM), Dasatinib (Inhibits ABL and SRC family kinases, 100nM) or SU6656 (potent SRC inhibitor with no activity against ABL, 1μM). γ-catenin was pulled down using Strep-Tactin and analyzed for tyrosine phosphorylation. To measure cell death: Ph^+ cell lines were treated with Imatinib (1μM),

Nilotinib (100nM), Dasatinib (100nM) and SU6656 (1μM). Apoptosis was analyzed after 12 hr or 24 hr using flow cytometry for Annexin versus 7-AAD.

BCR-ABL1-Positive and Negative Human Cell Lines

Cell Line	Stage[a]	Translocation mut/WT	*IKZF1*[a,b]	*CDKN2A/B*[c]	PAX5[d]	IC_{50} Imatinib (nM)[a]	IC_{50} Dasatinib (nM)[a]
NALM-1	B BC	BCR-ABL1; p210; WT[a]	Δ/WT IK6$^-$	Δ		>10000	>1000
SD-1	B Lymp	BCR-ABL1; p190; WT[a]	IK6$^-$			>10000	n.d.
Sup-B15	pre-B	BCR-ABL1; p190; WT[a]	Δ3–6/WT IK6$^+$	Δ	WT	2000	100
BV-173	B BC	BCR-ABL1; p210; n.d.[a]	IK6$^+$	Δ	WT	100	100
TOM-1	pre-B	BCR-ABL1; p190; n.d.[a]	Δ3–7/WT IK6$^-$			80	n.d.
K562	M BC	BCR-ABL1; p210; n.d.[a]		Δ	WT	200	n.d.
REH	pre-B	ETV6-RUNX1			WT		
Sem	pre-B	MLL-AF4					
697	pre-B	TCF3(E2A)/PBX1			WT		

B BC, B cell blast crisis; B Lymph, B lymphoblastoid; M BC, Myeloid blast crisis; mut, mutated; WT, wild-type; n.d., not determined; Δ, deletion, IK6: expression of the dominant-negative Ikaros (*IKZF1*) splice variant 6.

[a](Quentmeier et al., 2011).

[b](Mullighan et al., 2008).

[c](Feldhahn et al., 2007).

[d]http://cancer.sanger.ac.uk/cell_lines/gene/overview?ln=PAX5.

shRNA Assays

Cells were infected with lentivirus based vectors (pLKO) containing specific hairpins to human γ-*catenin* (TRCN0000083709 (Sh JUP1) and 83710 (Sh JUP2)), human β-*catenin* (TRCN0000003843 and 3845) (Open Biosystems) and human *MYC* (TRCN0000174055 and 10390) or a scrambled sequence (Sh scr) as a negative control (SHC002, Sigma). Forty-eight hr post infection, the cells were selected in puromycin. Three days later, puromycin resistant cells were re-plated and live cells were counted every two days and analyzed by Western blot and cell cycle/apoptosis analysis was done using Hoechst staining.

Sup-B15 cells were transduced with sh RNA constructs (Sh JUP2 or Sh scr) and puromycin-resistant cells were transplanted (i.v.) into sub-lethally (375 cGy) irradiated NOD *Prkdc*^{scid} *Il2rg*$^{-/-}$ (NSG) mice (2*10^6/mouse). Two weeks later mice were sacrificed and the presence of human cells was assessed by flow cytometry for human β2 microglobulin (β2m) relative to mouse CD45.

Primary Human Ph$^+$ B-ALL Samples

All primary ALL samples were derived from leftover diagnostic samples from patients that were enrolled in multicenter trials on treatment of pediatric ALL conducted by individual member groups of the AIEOP-BFM study group (Austria, Germany, Italy and Switzerland). All treatment trials were approved by the respective national institutional review boards, and informed consent for the use of spare specimens for research was obtained from study individuals, parents or legal guardians. Approval for experiments with human samples in the mouse xenograft model to study disease mechanisms was obtained from the ethics commission of the Canton Zurich (approval number 2014-0383). Animal experiments were approved by the veterinary office of the Canton of Zurich, Switzerland.

To obtain xenografts, primary ALL cells were recovered from cryopreserved samples and transplanted intrafemorally to NSG mice as previously described (Schmitz et al., 2011). Leukemia progression was monitored by flow cytometry with rat anti-mouse CD45 (eFluor450, clone 30-F11, REF 48-451-82, eBioscience), mouse anti-human CD45 (Alexa Flour 647, clone HI30, REF 304018, BioLegend), and mouse anti-human CD19 (PE, clone HIB19, REF 302208, BioLegend). ALL cells recovered from spleens of NSG mice were used for experiments.

Thawed patient derived Ph$^+$ B-ALL cells were cultured overnight in Opti-MEM supplemented with 10% FCS, 10mM HEPES, 1% penicillin-streptomycin, 10 ng/ml of IL-7 and 10% of WEHI-3B supernatant (5x10^6 cells/ml).

For γ-catenin knockdown, we subcloned the above used hairpins to human γ-*catenin* Sh JUP1 (TRCN0000083710) and Sh JUP2 (TRCN0000083711) and the scrambled sequence (Sh scr, SHC002) together with the hU6 promoter from the pLKO into Lentivirus backbones containing hPGK-GFP or -Cerulean followed by a WPRE element.

After overnight pre-stimulation, the patient derived Ph$^+$ B-ALL cells were infected with fresh concentrated supernatant containing Sh JUP or Sh scr Lentivirus in the presence of polybrene (5 μg/ml) for 4 hr and the infection was repeated the next day. After the second infection, the two populations of transduced cells were mixed 1:1 and injected into NSG recipient (10^6 cells/mouse). A small fraction of cells was kept in culture for 2-6 days to determine the rate of transduction by flow cytometry.

Characteristics of B-ALL Patient Samples

	Mouse no.	Sample ID	BFM ID	Risk	Karyotype	Treatment Response	Relapse
Patient#1	m3292		B73	MR	BCR-ABL, hyperdiploid	Prednisone Good Response	CNS relapse
Patient#2	m3293	ZH04		SR	BCR-ABL	Prednisone Good Response	

Pull Down and Western Blots

Cells were lysed RIPA buffer (50 mM Tris-Cl pH 7.4, 150 mM NaCl, 1%NP-40) containing Phospho Stop and Protease Inhibitor Cocktail (Roche) for 30 min at 4°C. The cleared protein extract was incubated with Strep-Tactin Sepharose beads (IBA) for 15 min at 4°C. Beads were washed 3x in lysis buffer and proteins were eluted for 15 min at 4°C using lysis buffer containing 50mM Biotin (Sigma). Supernatants were analyzed by Westerns blots.

For Western blots, cells were lysed in Laemmli buffer (BioRad) and lysates were boiled for 10 min before running on 10% acrylamide gels (BioRad). After transfer to nitrocellulose (Bio-Rad), membranes were saturated using TBS with 5% milk or 0.5% gelatin for 1 hr and incubated with primary antibodies overnight followed by appropriate secondary antibodies coupled to HRP (Horseradish peroxidase) (see Key Resources Table) for 45 min and developed using standard ECL (GE Healthcare) or Femto ECL (Thermo Scientific). Signals were visualized using X-Ray films (Fuji) and quantified using ImageJ software (NIH).

Chromatin Immunoprecipitation (ChIP)

Sup-B15 and K562 cells were crosslinked using a two-step method. In brief, nuclei were extracted, lysed in 10mM Tris pH8, 0.3% SDS, 1mM EDTA, 0.5mM EGTA and sonicated to 500bp average length using a Covaris S2 sonicator. The sonicated cell lysate was clarified by centrifugation, diluted 8x in IP buffer (10mM Tris pH8, 160mM NaCl, 1mM EDTA, 1% NP-40, 0.1% sodium deoxycholate) and incubated with anti-γ-catenin (BD 610253), anti-β-catenin (Santa Cruz sc-7199) or control rabbit IgG (Millipore 12-370) antibodies pre-coupled to magnetic beads (Lifetechnologies 10001D, 10003D) over night. Complexes were washed in low (150mM NaCl, 20mM Tris pH8, 1% sodium deoxycholate, 1% NP-40, 1mM EDTA) and high (500mM NaCl, 20mM Tris pH8, 1% sodium deoxycholate, 1% NP-40, 1mM EDTA) salt buffers, eluted in 25mM Tris, 10mM EDTA, 1% SDS for 30 minutes and de-crosslinked at 65°C for 7 hr. Following proteinase K and RNAse treatment, DNA was purified using the Qiagen MinElute PCR purification kit. The relative amount of immunoprecipitated DNA fragments was quantified by qPCR on input and IP samples and enrichment calculated by normalizing with IgG control values and dividing by enrichment at control loci located upstream of either *MYC* or *AXIN2*. Five conserved Tcf/Lef-binding elements at the *MYC* locus (He et al., 1998; Kolly et al., 2007; Yochum et al., 2008) were amplified as well as a Tcf/Lef binding element of an upstream enhancer that interacts with the *MYC* promoter (Pomerantz et al., 2009; Tuupanen et al., 2009). At the *AXIN2* promoter two Tcf/Lef binding elements were amplified (Jho et al., 2002).

ChIP for HA tag: Sup-B15 cells were cross-linked in 1% formaldehyde (Thermo scientific, Ref: 28908), at 37°C for 10 min. The reaction was quenched with 125mM glycine, followed by 2 washes in ice-cold PBS (supplemented with protease/phosphatase inhibitors (1x PIC)). Fresh or frozen cell pellets were re-suspended in ChIP-lysis buffer (0.3% SDS, 50 mM Tris (pH 8.1), 10 mM EDTA (pH 8.1), 1x PIC) and chromatin was sonicated to an average length of 200-500bp using a sonicator (Branson Sonifer 250). The sonicated cell lysate was clarified by centrifugation, diluted 9x in ChIP dilution buffer (0.01% SDS, 1.1% Triton X-100, 1.2 mM EDTA, 16.7 mM Tris-HCl (pH 8.1), 167 mM NaCl, 1xPIC) and $20x10^6$ cell equivalents of chromatin was pre-cleared with BSA-coated Protein A+G magnetic beads (Millipore 16-663) for 4 hr at 40°C, and then incubated overnight with anti-HA antibody (ab9110) coupled Protein A+G magnetic beads or beads alone.

Immune complexes were in washed once each in low (0.1% SDS, 1% Triton X-100, 2 mM EDTA, 20 mM Tris-HCl, pH 8.1, 150 mM NaCl, 1x PIC) and high (0.1% SDS, 1% Triton X-100, 2 mM EDTA, 20 mM Tris-HCl, pH 8.1, 500 mM NaCl, 1X PIC), and LiCl salt buffers (0.25 M LiCl, 1% IGEPAL CA630, 1% deoxycholic acid (sodium salt), 1 mM EDTA, 10 mM Tris, pH 8.1, 1X PIC), and twice in Tris-EDTA (10 mM Tris-HCl, pH 8.0, 1 mM EDTA), prior to two elutions in 1%SDS, 0.1M $NaHCO_3$ for 30 min at 65°C, and de-crosslinked at 65°C overnight. Following proteinase K treatment at 55°C for 2 hr, DNA was purified by phenol-chloroform extraction and ethanol precipitation. The relative amount of immunoprecipitated DNA fragments was quantified by qPCR on input and IP samples using primers listed in the Key Resources Table and enrichment was calculated by normalizing to beads alone control values.

Data Analyses

Comparisons between two groups were performed using Student's t tests (two tailed) and between multiple groups by ANOVA (Bonferroni post-hoc). A Mantel-Cox test with 95% confidence interval was used to compare survival curves. Significant differences between data sets are indicated by * $p < 0.05$, ** $p < 0.01$, *** $p < 0.001$. ns not significantly different ($p>0.05$).

DATA AND SOFTWARE AVAILABILITY

The accession number for the array data reported in this paper is GEO: GSE54793.